EUROPEAN COMMISSION CONTRACT No. HPRI-CT-1999-50001

APPENDIX B

The Driver Accelerator for EURISOL

REPORT OF THE

DRIVER ACCELERATOR TASK GROUP

December 2003

APPENDIX B

The Driver Accelerator for EURISOL

REPORT OF THE
DRIVER ACCELERATOR TASK GROUP

Co-ordinator: Alex Mueller

Report to the European Commission
EUROPEAN COMMISSION CONTRACT No. HPRI-CT-1999-500001

The report of the EURISOL Driver Accelerator Task Group was mostly completed before the end of 2002, and any subsequent developments in the field are therefore not reflected in this document.

Edited by John Cornell
Technical Co-ordinator, EURISOL Project

Published by GANIL
BP 55027, 14076 Caen cedex 5, France
December 2003

Contents

1 Introduction

This report is the result of the work done by the Driver Accelerator Task Group of the EURISOL RTD project. Accelerator experts from the laboratories [1] participating in this study, namely CEA-Saclay, CERN, GANIL, INFN Legnaro and IPN Orsay, have investigated various different technical solutions during the period 2000–2001, following the specifications recommended by the EURISOL Steering Committee.

1.1 Definition of the task

EURISOL aims at making radioactive ion beams of intensities which will be several orders of magnitude greater than those available at present-day accelerator facilities. In order to achieve this, it is clear from the outset that the driver accelerator needs to deliver very intense beams to the production target, notwithstanding the importance of the efficiency optimisation of the later stages in the ISOL and post-acceleration processes.

The scope of the task for the Driver Accelerator Task Group thus encompassed:

- **investigation of various solutions for a high-intensity driver accelerator, based on existing projects, current R&D and new and foreseeable developments;**
- **assessment of the best technical solution;**
- **estimation of costs and performance/cost optimisation;**
- **identification of future R&D needed to bring such a project to fruition; and**
- **identification of any possible synergies with other European projects or planned facilities.**

1.2 Method of work

At the early Steering Committee meetings, it became apparent that the working specifications for the driver accelerator could only be defined after the initial studies by the Key Experiments Task Group and the feed-back by the user community at the first EURISOL town meeting (at Orsay, on November 6th & 7th, 2000). Up to that point, preparatory work in the laboratories [1] involved focused on generic studies and developments of high-intensity accelerator components suitable for EURISOL. In parallel, possible synergies with other high-intensity projects were also investigated (see, e.g. http://conference.kek.jp/SRF2001/).

The Driver Accelerator Task Group then convened a first formal meeting which took place on the 20th November 2000, when specific tasks were allocated. Two further meetings permitted monitoring and co-ordinating of the ongoing work. Regular progress reports were made at the Steering Committee meetings. The suggestions arising from the Steering Committee members were referred back to the task group.

The working documents – presentations and preliminary reports – of the task group meetings have been available to the community via the EURISOL website (http://www.ganil.fr/eurisol). An editorial subgroup synthesised the various documents and studies into a final draft report. This draft document was presented to the meeting of the full Task Group on the 12th October 2001 for discussion and approval.

1.3 Different options for driver particle beams

The objective of the EURISOL is the preliminary design study of the next-generation European ISOL facility, which is ***complementary to*** a future European Heavy-Ion facility relying on In-Flight Projectile Fragmentation around 1 GeV/u energy and intensities of 10^{12} pps. EURISOL aims at the optimal exploitation and extension of ISOL technology, thus providing radioactive ion beams that are ***orders of magnitude higher in intensity*** than those which are presently available. In the light of this general objective and the inherent limits imposed by practical target considerations, the Steering Committee proposed the following driver options:

- **a high-intensity 50-MeV electron accelerator** (20-30 mA), to provide photo-fission products from bremsstrahlung, as the example of a low-cost solution for a dedicated region of the isotopic chart;
- **a high-intensity 1-GeV proton accelerator**, operated in two intensity regimes. At intensities around a few hundred μA it would be operated as a classical ISOL facility. The full beam power (approximately 5 MW) would be used to generate neutrons from a spallation target, which in turn are used for producing fission products (the so-called 'converter method');
- **a high-intensity proton accelerator** with ***heavy-ion capability*** for low-mass species, with ion beam powers of hundreds of kW, because of current interest in some selectivity and cross section properties of heavy-ion induced reactions.

These options were studied under the assumption that EURISOL would be stand-alone facility. The studies then provide a baseline to which other driver accelerator configurations can be referred.

1.4 Synergies and duty-cycle considerations

Synergy between the EURISOL driver accelerator and other projects has, of course, to be taken into account. In order to avoid duplication of efforts and a rationalisation of resources, it is necessary to investigate all possible links and synergies. Indeed, the design of high-power accelerators is of great current interest in several other scientific projects. Various levels of synergy between different projects can be envisaged:

- **interchange of information and experience;**
- **sharing of computer codes and capitalising on common design goals;**
- **collaborating on common R&D of dedicated components;**
- **adoption of major hardware developed by another project;**
- **design and manufacture of accelerator sections together with other project teams;**
- **construction of a dual-purpose (or even multi-purpose) driver accelerator.**

Other high-intensity proton accelerators with energies in the GeV region at present being designed, developed or proposed – and with which synergies could be envisaged – are:

- **neutrino (and muon) factories**. The CERN community is studying such a facility [2] based on a 4-MW linac.
- **accelerator-driven hybrid reactor systems**. This concept has been proposed in Europe [3], the USA [4] and in Japan [5] for nuclear waste incineration. The

'European Roadmap' [6] prepared by the Technical Working Group (TWG) quotes the 10-MW level for a demonstration facility and the 50-MW level for the industrial extrapolation.

- **spallation neutron sources** for material science, presently under construction in the US (SNS [7]) and Japan (Joint Project [8]), or planned in Europe (ESS [9]). These projects use multi-MW power linac accelerators.
- **technological irradiation tools** for the development of new radiation-resistant materials. These need neutron sources able to provide fluxes of some 10^{15} $n/cm^2.s$, corresponding to proton beam powers of the order of 10 MW.

The most powerful proton accelerators running at present are the Los Alamos linac and the PSI cyclotron. Beam power is, in both cases, about 1 MW. The considerable increase in beam power needed for the new projects is the driving force behind the present major R&D effort. ***The inherent energy limitation of the cyclotron, and the fact that the ultimate beam power limit is more than an order of magnitude higher for the linac, explains why the majority of these projects concentrate on a linac solution.*** The same arguments naturally apply to the EURISOL driver accelerator. For similar reasons, the concept of an FFAG-synchrotron* has also not been chosen for further investigation, although some interesting R&D is presently under way, mainly at KEK [10]. There they have recently built a proof-of-principle 0.5-MeV FFAG, and are now constructing a 150-MeV machine for further investigations, in particular in the context of hadron-therapy. However, at the present stage the concept is not yet sufficiently advanced for assessing it in the context of multi-megawatt beams and comparing to a linac solution, in particular with regard to transmission, reliability and cost.

Some of these projects have mandatory duty-cycle requirements, e.g. spallation neutron sources and neutrino facilities need pulsed beam because of their subsequent cyclic accelerators. For EURISOL the choice was not immediately clear. Because the power deposited in the radioactivity-releasing ISOL target is a major concern, the maximum smoothing-out of the beam structure is favoured. 'Wobbling' the driver beam over the target is most probably needed, which again favours a continuous time structure. Therefore, at least for a stand-alone facility, the Steering Committee recommended CW as the preferred mode of operation. The base solutions for the driver accelerators presented in this report are thus of the CW type. Nevertheless, a comparative study between pulsed and CW operation has been made and is reported in section 5. For measurements of target release properties, a sharp cut-off of the full beam power for quite variable periods of time is required, regardless of the mode of operation.

If EURISOL is to be incorporated in a dual-purpose (or multi-purpose) facility then the pulsed mode of operation might be a necessity. In that case, the pulse rate on the EURISOL target should exceed 50 Hz, for smoothing out the thermal load on the target.

* Fixed-Field Alternating-Gradient Synchrotron. This allows a much higher cycling frequency than that of a classical synchrotron with a time-varying magnetic field. Accordingly, the intensity can, in principle, be increased by more than an order of magnitude compared to a (rapid-cycling) synchrotron.

2 An Electron Driver Accelerator

The baseline option for the EURISOL driver accelerator is a 1–2-GeV proton linac. At reduced power levels, various proton-induced reactions provide access to a large variety of species in the nuclear chart, whereas at the full power level of 5 MW, this driver is used as spallation neutron generator for the creation of fission products.

Another possibility for a fission-based radioactive beam facility is the use of a low-energy (50–100-MeV) electron driver, using 'photo-fission' of ^{238}U: the bremsstrahlung generated by the electron-beam-induced GDR (Giant Dipole Resonance) excitations in the uranium target, leading to creation of neutrons and fission products. The fission cross section of ^{238}U reaches its maximum for 15-MeV photons [11], and simulations made by Y. Oganessian [12] and by D. Ridikas [13] show that a 50-MeV electron can create about 6×10^{-3} fissions (see figure 2.1). Note that these first simulations were confirmed in April 2001 during the test experiment PARRNe-1 at CERN [14].

The promise of photo-fission lies in the fact that intense 50-MeV electron beams can be made for comparatively modest investments, as discussed below. There is currently much interest in that technique, e.g. the Flerov Laboratory in Dubna has selected it for an upgrade of their facility, and GANIL in Caen has discussed it as an option for the future SPIRAL-2 project [15].

However, this solution may not reach the same ultimate RNB luminosity as that obtained through fast-neutron-induced reactions: the 'energetic' neutron cost is an order of magnitude higher for photo-fission than for spallation, and the resultant mass and charge distribution may be narrower [16]. But note, however, that while the fast-neutron-induced reactions have considerably higher yields for nuclei in the symmetric fission region (Z = 65 – 80), the release properties of these refractive species are highly problematic. On the other hand, photo-fission is similar to 'cold' neutron-induced fission and thus produces more exotic nuclei as opposed to the 'hot' fission where the neutron evaporation of the excited fission drives the final reaction product back towards stability.

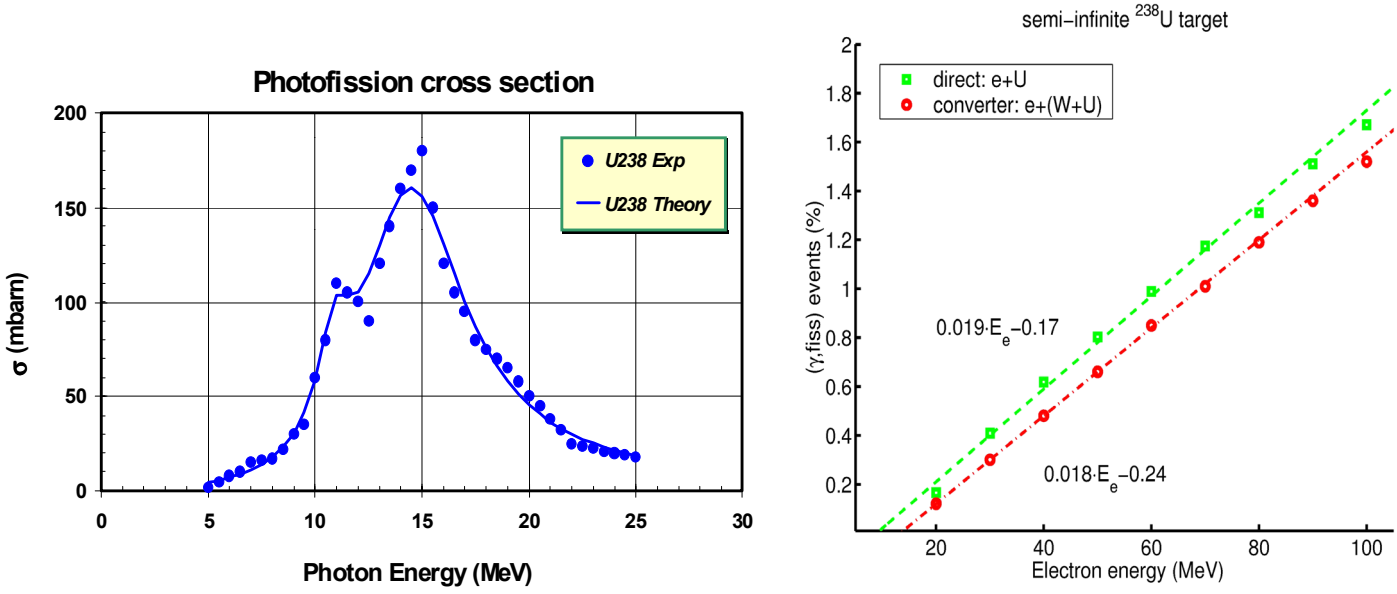

Fig. 2.1: (Left:) Photo-fission cross section for ^{238}U. (Right:) Number of fission per incident electron as a function of electron energy for the direct method (^{238}U) and the converter method (5 mm W + ^{238}U).

2.1 Specifications of the electron driver accelerator

The stated goal for a EURISOL electron driver is to induce more than 10^{15} fissions/s in the uranium target (ignoring for the moment the issue of power density deposition in the target). This goal leads to beam specifications as follows:

- **Final beam energy: 50 to 70 MeV.**
- **Average beam current: 20 to 30 mA.**

In order to create this 1- to 2-MW electron beam, a high-power CW superconducting linac was considered. This choice presents many advantages:

- ***optimal efficiency***, with almost 100% of the RF power transmitted to the beam, despite the use of cryogenics;
- ***reduced overall length*** because high accelerating gradients reduce the number of accelerating structures needed;
- ***flexibility*** provided by the ease of changing beam energy and current;
- ***reduced activation*** of the accelerating structure from beam halos because of the large apertures of the cavities;
- ***reliability*** since CW operation allows lower peak current.

Note that this driver can be considered as an 'up-graded' version of the SPIRAL-2 electron driver option (45-MeV, 500-μA beam) which aims to create about 2×10^{13} fissions/s in the target [17].

2.2 The electron linac

The proposed layout of this electron linac is very simple (see figure 2.2): an injector, composed of an electron gun at about 100 kV followed by a capture cavity, accelerates the beam up to 5 MeV; a subsequent β=1 section increases the energy to 50 MeV. The overall length of such a machine is about 20 m.

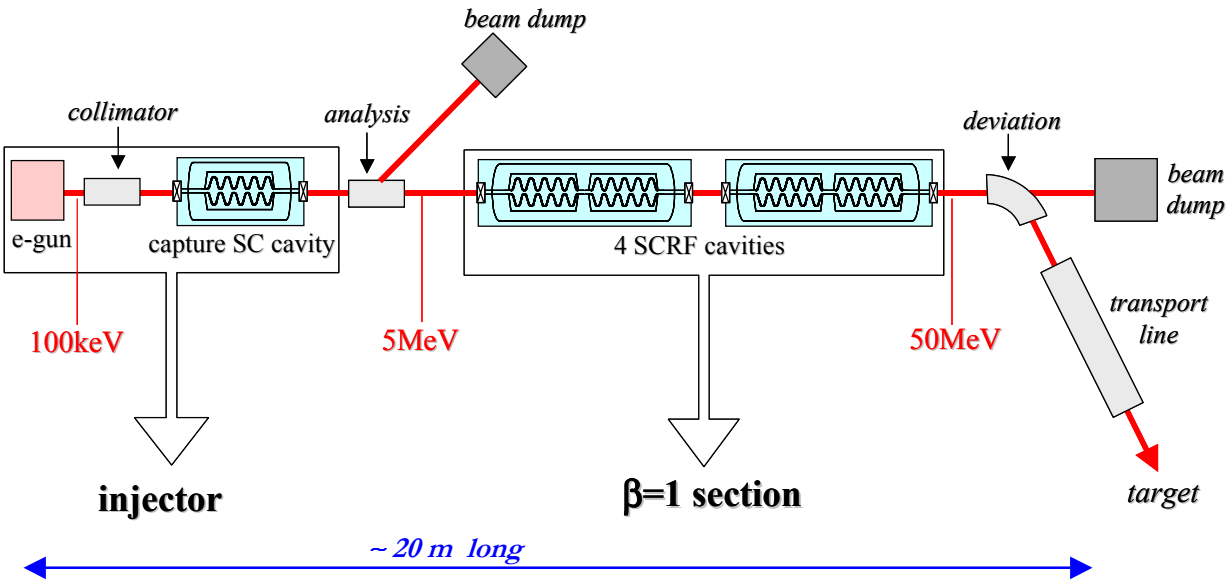

Fig. 2.2: Proposed layout of the electron linac.

2.2.1 The injector

The injector is designed to produce a quasi-relativistic electron beam (about 5 MeV), bunched to the desired frequency, and with acceptable emittance. It is composed of:

- ***a high-current electron gun*** (a few tens of mA); e.g. a gridded triode with modulation of the cathode for bunching (note here that depending on the e-gun bunching performances, a specific pre-bunching cavity could be needed after the gun);
- ***a collimator system*** to control the beam emittance; and
- ***a possible capture cavity*** to accelerate the beam up to a few MeV with large energy and phase acceptance.

Two main alternatives can be envisaged for such an injector (figure 2.3). First, a 'high-energy' gun can be used to produce electrons of more than 250 keV (β~0.75). In this case, no special capture cavity is needed since a β=1 superconducting cavity can directly follow the gun for capture. However, the technical realisation of such a high-energy gun could become quite complicated and/or expensive.

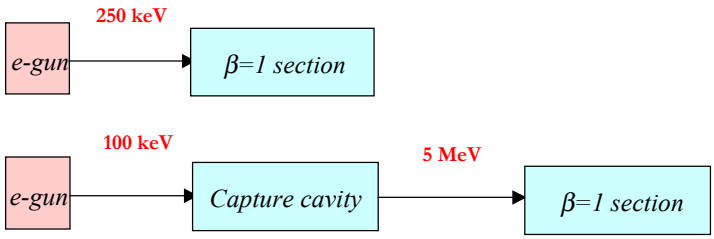

Fig. 2.3: Two alternative schemes for the injector section.

The second solution, which may be easier to realise, consists of a 'low energy' gun, providing electrons of 100 keV (β~0.55). In this case, a special superconducting cavity would have to be developed for efficiently capturing the 100-keV electrons and accelerating them up to 5 MeV with acceptable energy and phase dispersions.

A preliminary study has been started on this item using RF codes like SUPERFISH in both SPIRAL-2 and EURISOL contexts. Two variants of 5-cell prototypes have been designed (figure 2.4), aiming to capture 100-keV electrons: the first one is a 5-cell β=0.85 cavity, the second one is a 'hybrid cavity', composed of two β=0.8 cells followed by three β=1 cells.

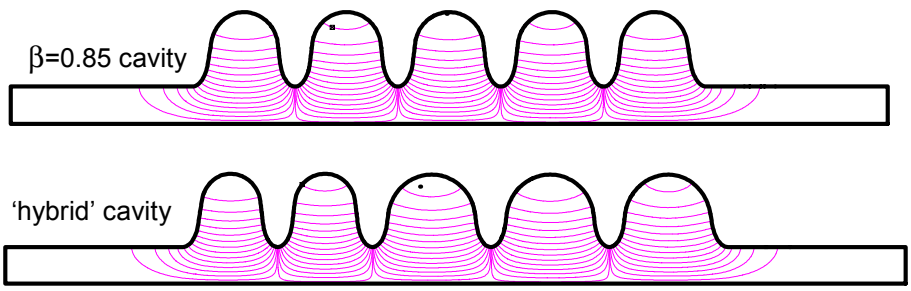

Fig. 2.4: SUPERFISH calculations of the electromagnetic field for two variants of a capture cavity. Only the upper half of the 5-cell structure is plotted in each case.

For an operation with a conservative value of the peak surface magnetic field B_{pk} = 50 mT ($E_{acceleration} \approx 12$ MV/m), the energy of the electrons leaving the cavity is about 4.5 MeV, and reaches more than 7 MeV at B_{pk} = 80 mT ($E_{acceleration} \approx 20$ MV/m). Figure 2.5 represents the evolution of the energy of an electron entering the two cavity variants at optimal phase. The case of a 5-cell β=1 cavity is given for comparison. These calculations have been made taking into account the stray field at both ends of the cavity; note that these stray fields create unwanted but unavoidable deceleration at the entrance of the cavity.

An important issue in this study is the phase acceptance of the capture cavity. It has been calculated (figure 2.6) that the higher the accelerating field, the narrower the phase acceptance. At B_{pk}=50 mT, the phase acceptance of our cavities is about 90°.

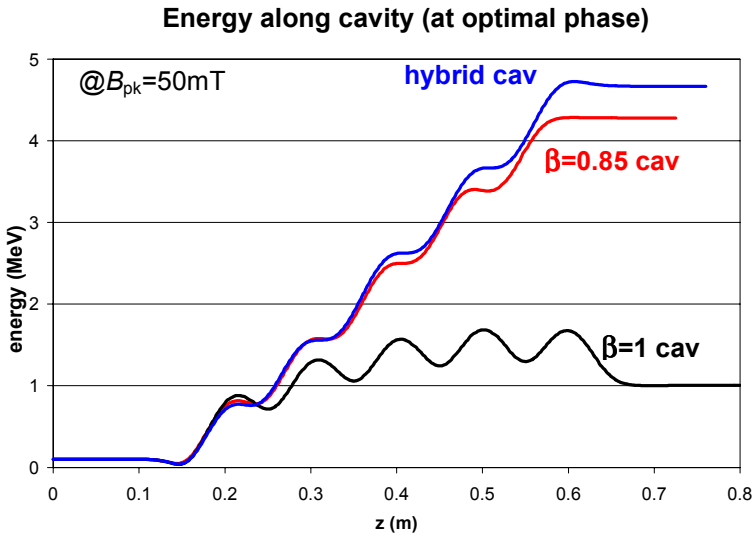

Fig. 2.5: Comparison of the electron energy along the capture cavity for the two proposed variants. These have been calculated for a frequency of 1.5 GHz. In addition it is shown that a β=1 cavity is not useable because of phase mismatching.

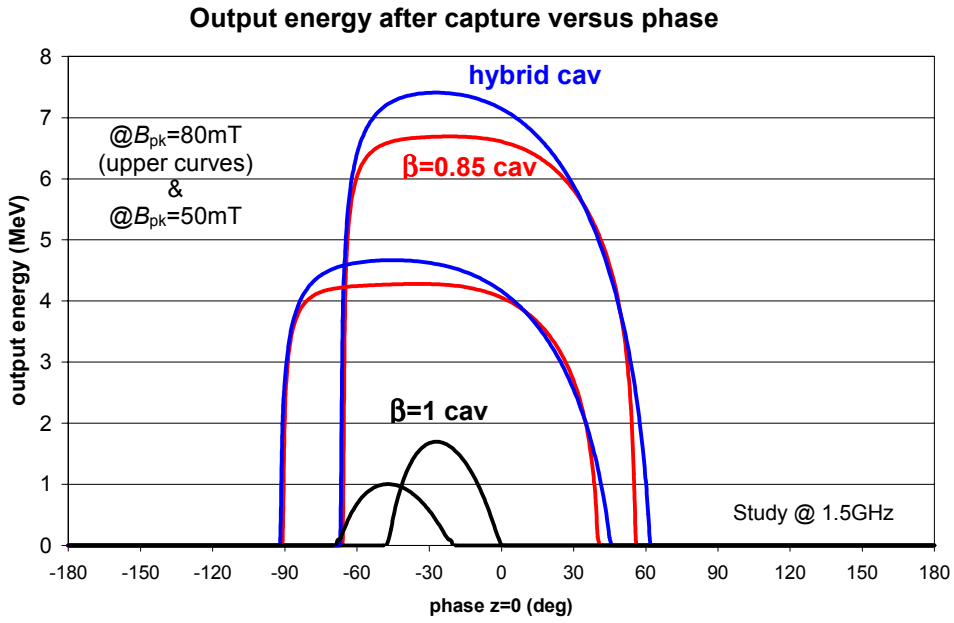

Fig. 2.6: Phase acceptance of the two capture-cavity variants for two selected magnetic peak fields, and a β=1 cavity for comparison.

Finally, preliminary simulations show (figure 2.7) that our designed capture cavities have very good bunching properties: all the particles injected from a 100-keV bunch of 30° phase dispersion (and 200-eV energy dispersion) are contained after capture (at ~4.5 MeV) within less than 5°, and with an energy dispersion less than 40 keV. Such a cavity is also expected to exhibit transverse focusing properties that have not yet been studied.

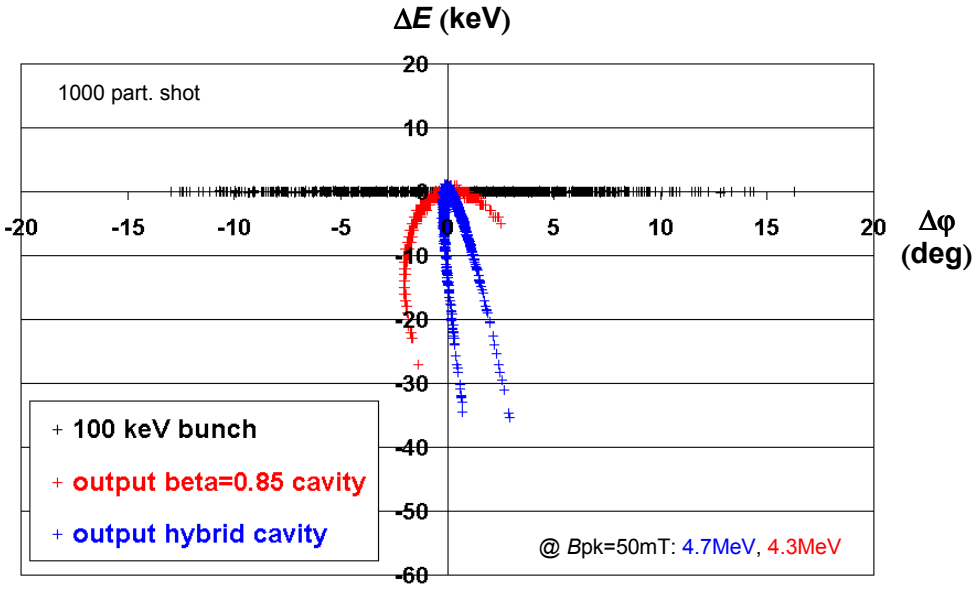

Fig. 2.7: First simulation of the output characteristics (phase and energy dispersion) of the two capture cavities which were investigated.

2.2.2 The β=1 section

The β=1 section of the electron driver would have to accelerate the beam from 5 MeV to 50 MeV (or even higher). Given the typical characteristics for a β=1 cavity ($B_{pk}/E_{acc} \approx 4$ mT/(MV/m) and $E_{pk}/E_{acc} \approx 2$), it appears that this goal can easily be reached using 4 superconducting cavities:

- In the case of a 'basic' 50-MeV 20-mA driver (1-MW beam), the energy gain needed is thus 11.25 MeV per cavity. This leads, in a 700-MHz 5-cell cavity or in a 1.3-GHz 9-cell cavity, for example, to an operation at peak magnetic surface fields of about $B_{pk} \approx 45$ mT, which is a very safe value. The RF power needed is about 225 kW per cavity.
- This basic driver can even be upgraded to produce a 70-MeV 30-mA beam, raising the energy gain per cavity to 16.25 MeV; this would raise the peak magnetic surface field up to $B_{pk} \approx 65$ mT, which can still be reached quite easily. The RF power needed per cavity is here about 490 kW.

The design of β=1 SCRF elliptical cavities operating with such accelerating gradients is now a technology which has proven to be quite well mastered, especially thanks to the successful development of the CEBAF cavities at 1.5 GHz and of the TESLA cavities [18] at 1.3 GHz.

A major consideration is the very high RF power needed in each cavity (200 to 500 kW CW). Apart from RF power source requirements, the most important point is the impact on the power coupler: the development of a 500-kW CW power coupler is actually a real technological challenge. However, it is subject to ongoing R&D at several laboratories. Recent advances have been made at KEK in Japan (the 500-MHz KEK-B power coupler is in routine operation at

380 kW CW), at Cornell and Los Alamos in the US (the 700-MHz APT power coupler reaches 1 MW CW at room temperature and 500 kW when cooled at nitrogen temperature), and at CERN in Europe (the 350-MHz LEP-2 coupler reaches 500 kW CW on a test stand). An alternative would be to increase the number of cavities or to add a second cryomodule.

2.2.3 Elements affecting the choice of frequency

Superconducting electron accelerators presently operating work in the 500 MHz – 1.5 GHz frequency range (except LEP at CERN at 352 MHz and S-DALINAC at Darmstadt at 3 GHz), owing to limitations imposed by the physics of RF superconductivity.

For the small size of the electron driver discussed here, where only a few cavities are needed, the final frequency will be determined mainly by the availability of existing RF components, which would reduce both the R&D effort and the total driver cost. The SPIRAL-2 study for example chose an RF frequency of 1.5 GHz in order to benefit from most of the existing components of the decommissioned Saclay superconducting linac MACSE [19].

In order to benefit from the ongoing developments on other projects, three possible frequencies are discussed here: 350 MHz (CERN-LEP), 700 MHz (European proton drivers and the American APT/AAA), and 1.3 GHz (TTF/TESLA). Note in this context that the high-energy section of the proposed EURISOL proton driver would use 700 MHz (see section 3.3). A comprehensive summary of the existing potential at these frequencies is presented in table 2.1.

A very preliminary study comparing β=1 sections for a EURISOL electron driver operating at different frequencies is shown in table 2.2. Better efficiency and shorter length are reached by operating at 700 MHz or at 1.3 GHz. The choice of 350 MHz frequency is penalised, both in terms of efficiency and length: the β=1 section's overall length exceeds 20 metres at 350 MHz, whereas at 700 MHz or 1.3 GHz, it stays below 10 metres. However, availability of equipment and expertise at 350 MHz due to the development of this technology for LEP could outweigh the intrinsic drawbacks of such a low frequency.

Table 2.1: Potential sources of RF Components.

Frequency	350 MHz	700 MHz	1.3 GHz
Electron gun	→ LIL thermionic guns *(current increase needed)*	*(Non-existent at present)*	→ TTF injector 1 40 kV gun + 300 kV electrostatic column, 1mA CW, 216.7 MHz *(current increase needed)*
SC cavities	→ LEP 4-cells β=1 cavity	→ big R&D effort going on for proton cavities. *(easily applicable to electron cav.)*	→ TTF 9-cells β=1 cavity
RF CW power couplers	→ LEP coupler: design power = 210 kW	→ AAA/APT coupler: design power = 210 kW, >500 kW on test stand at 70K	To be developed *(from TTF couplers 200 kW peak - 1.5 kW average ?)*
RF CW power supplies	→ LEP 1.1 & 1.3 MW klystrons	→ AAA/APT 1 MW klystrons → Thalès IOT 80 kW *(300 kW to be developed)*	Easy development from Thalès 10 MW peak – 250 kW average – klystrons

Table 2.2: Main parameters for a proposed EURISOL β=1 section at different frequencies (20 mA, 5–50 MeV). The total AC efficiency is obtained by assuming an AC-to-RF conversion factor of 60%, and cryogenic efficiencies of 0.1% at 2 K and 0.3% at 4.5 K, respectively.*

Frequency	350 MHz	700 MHz	1.3 GHz
No. of cavities needed	8 (4-cells) in 2 LEP modules	4 (5-cells) in 1 module	4 (9-cells) in 1 module
Operating accelerating field	3.3 MV/m	10.5 MV/m	10.8 MV/m
Section length	25 m	7 m	7 m
Total RF power needed	0.9 MW	0.9 MW	0.9 MW
Operating Q_o	2.10^9	1.10^{10}	5.10^9
Total thermal load	760 W @ 4.5K	130 W @ 2K	140 W @ 2K
Total AC efficiency	51.3%	55.3%	54.8%

* Easily upgraded to 30 mA, 5–70 MeV, just by raising the input RF power.

2.3 Preliminary cost estimate

A preliminary cost estimate has been made for a 50-MeV 20-mA electron driver, upgradeable to 70 MeV, 30 mA, running at a frequency of 700 MHz. Table 2.3 shows the estimated investments needed for the main components (infrastructures and buildings included, manpower not included). The cost of operation was evaluated considering operation at 65 MeV 20 mA (1.3-MW power and 1.3×10^{15} fissions/s produced in the uranium target), which simulates the upgrade at mid-life.

Table 2.3: Estimated Investment and Operating Cost for the electron driver.

INVESTMENT COST (including contingencies)	(M€)
Cryomodules	3.40
Injector	1.35
RF sources (IOT)	4.10
Cryogenics	5.45
Other (control systems, vacuum, etc.)	0.45
Total Component Cost	**14.75**
Infrastructures (for test & assembly)	1.45
Buildings	4.20
Total Investment Cost	**20.4**
OPERATION COST per year (80% operation time)	**(M€/year)**
Electricity cost	1.5
Staff and maintenance (rough estimate)	*~2.3*

2.4 Summary of the main features

This study shows that an electron driver with the specified characteristics is a machine that can be built fairly easily and rapidly since the extrapolation from the present state of the art requires only limited R&D efforts. Such an electron accelerator has several highly attractive features:

- The accelerator is very compact (about 20 m total for 700 MHz or 1.3 GHz technology).
- The activation of the accelerator structure should be relatively low, compared to a machine using protons and in particular deuterons for neutron production.
- The overall investment of 20 M€ (15 M€ without buildings and infrastructures) is an order of magnitude below that of, e.g., a 1-GeV proton driver.

However these advantages need to be weighed against the inherent power limitation, and consequent limits to achievable neutron fluxes, together with the limited range of radioactive species produced by photon-induced fission.

3 A Proton Driver Accelerator

A 5-MW proton driver accelerator is proposed for producing both neutron-deficient and neutron-rich exotic nuclei far from the valley of stability. It would be operated at full power as a spallation neutron generator for the subsequent production of neutron-rich nuclei by fission, and at a reduced power level (a few hundred kW) for direct proton-induced reactions (for proton-rich nuclei and light neutron-rich nuclei). The mean specifications of the proton driver accelerator in the EURISOL context are the following:

- **Final beam energy: 1 GeV, with a possible up-grade to 2 GeV.**
- **Average beam current: 5 mA for the main 5-MW '2-step' production mode (using a spallation target), and 0.2 to 0.5 mA for the 200- to 500-kW 'direct' production mode.**
- **Duty cycle: 100% (CW beam), while retaining the possibility of cycling the beam for life-time measurements (see discussion on operating mode in section 5).**

The general layout of such a proton driver is quite well-established, thanks to the numerous existing projects based on this kind of high-power linear accelerator. The specific layout proposed for the EURISOL proton driver accelerator is presented on the figure below. It is composed of three main sections:

1. **A low-energy section (up to 5 MeV) composed with a high-current proton source followed by an RFQ.**
2. **An intermediate section (from 5 MeV to 85 MeV) composed of super-conducting resonators (QWR or spoke-type) – or a room temperature DTL-like alternative.**
3. **A high-energy section (from 85 MeV to 1 or 2 GeV) composed of super-conducting elliptical multi-cell cavities of 3 different types.**

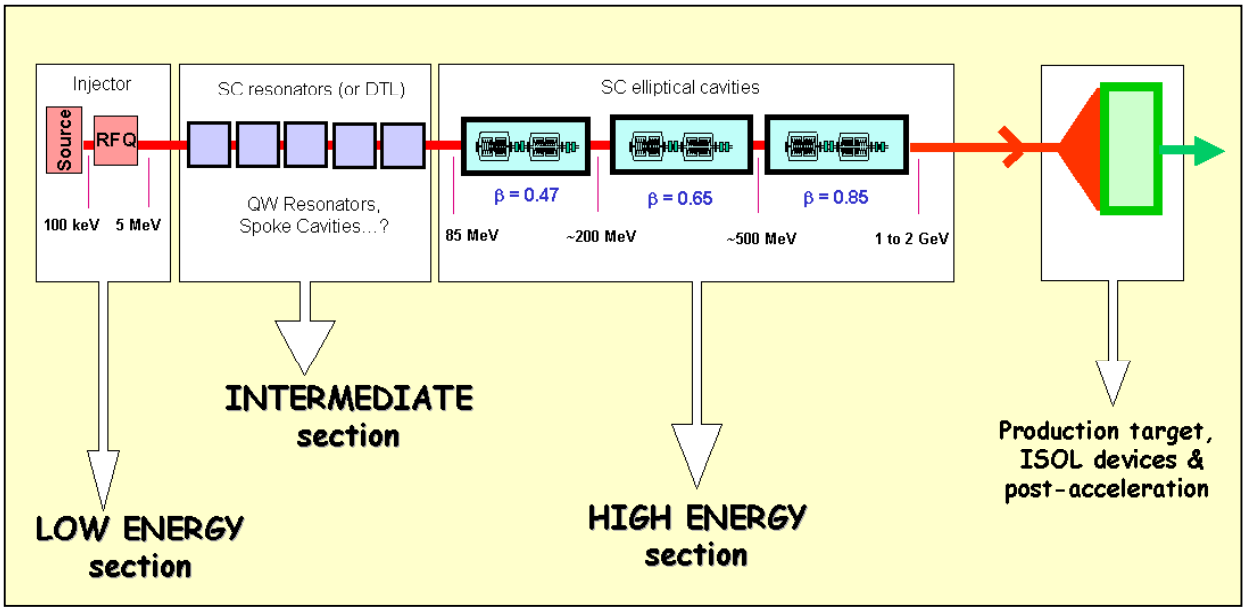

Fig. 3.1: General layout of the EURISOL proton driver accelerator.

3.1 The low-energy section (the injector)

For this study of the injector accelerator for the EURISOL 1–2 GeV proton driver, a room temperature copper RFQ structure fed by a high-intensity ion source has been adopted. Several laboratories are presently making huge R&D and construction efforts for such accelerators, which aim at ultimate intensities well above the EURISOL demand. The Los Alamos National Laboratory is the first to operate such an accelerator, LEDA [20], at intensities of the level of 100 mA DC. In Europe, the IPHI (Injecteur de Protons de Haute Intensité) project [21] is being undertaken in France by a CEA-CNRS collaboration, while in Italy, INFN is building an injector within the TRASCO (TRAsmutazione SCOrie) programme [22].

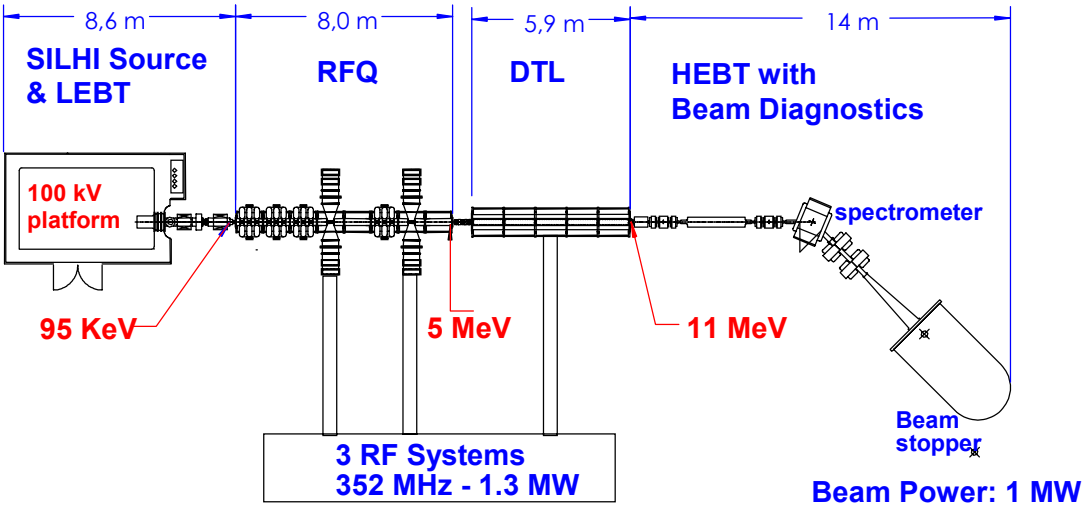

Fig. 3.2: Layout of the IPHI project.

IPHI is a 1-MW, 10-MeV demonstration accelerator consisting of an ECR proton source, an RFQ for beam energies up to 5 MeV, feeding a DTL accelerator and a subsequent analysing beamline (figure 3.2). The ECR source (SILHI, Source d'Ion Légers Haute Intensité, installed at Saclay), operating at 2.45 GHz with an ECR axial magnetic field of 87.5 mT, routinely delivers a 95-keV, 100-mA proton beam [23]. The source is driven by a 1.2-kW magnetron, but it will be replaced soon by a generator based on a 3-GHz, 1-kW klystron for better flexibility in pulsed mode. The design of the RFQ has been completed, and the beam dynamics has been studied using several complementary codes. The design of the vacuum system and the cooling system are practically completed. A cold model is in operation to validate the codes and optimise the RF tuning procedures.

Operating at a frequency of 352 MHz, the RFQ compresses the continuous beam from the source longitudinally into bunches ready for injection into the subsequent sections. The RFQ is optimised to provide a transmission of better than 95%, and has good optical properties in order to minimise beam loss in the subsequent structures. For achieving this goal, numerous technological challenges are being addressed, such as removal of the dissipated power (more than 100 kW/m), and fabrication techniques guaranteeing a dimensional accuracy and stability of 10 µm over the 8-m overall length. The RFQ will be fed by 1.8 MW of RF power (see table 3.1) provided by two 352-MHz, 1.3-MW klystrons (LEP type) through highly reliable windows and RF couplers (>250 kW). Finally, the design of the DTL has been completed, and construction of a short prototype tank is in progress; this model will test the technological choices, and permit validation of the RF codes as well as the magnetic measurements and alignment procedures.

Table 3.1: RF power needed for the 11-MeV IPHI injector.

Component	Beam current	50 mA	100 mA
RFQ	Dissipated power (copper)	1200 kW	1200 kW
	Beam loading	250 kW	500 kW
	Total RFQ power	**1450 kW**	**1700 kW**
DTL	Dissipated power (copper)	400 kW	400 kW
	Beam loading	300 kW	600 kW
	Total DTL power	**700 kW**	**1000 kW**

The injector of the TRASCO proton linac is more modest compared with IPHI (33-mA CW beam current instead of 100 mA), but is still well above the EURISOL specifications (5 mA CW). It is composed of a 2.45-GHz microwave-discharge ion source and a normal conducting 352-MHz CW RFQ up to 5 MeV. The TRASCO intense proton source (TRIPS) is fed by a 2.45-GHz 2-kW magnetron, and aims to produce at least a 35-mA 80-keV proton beam with an rms normalised emittance lower than 0.2π mm.mrad. The source was installed at INFN-LNS in May 2000, and it is now operational and has been able to deliver more than 20 mA of protons from a 5-mm hole at 65 kV extraction voltage [24]. The optimisation of the source is currently under way, with special care being given to reliability.

The design of the 7-metre long RFQ has been completed [25], and beam simulations show that beam transmission is expected to be more than 96% with losses mainly located below 2 MeV. The RF power will be provided by one single 352-MHz klystron with 1.3 MW nominal power (of the LEP type as in the IPHI case). Detailed design and engineering work has started and a 3-m long aluminium model of the RFQ has been built and measured for RF field stabilisation tests. Technological tests on a short copper section have been done and the first section of the RFQ is being constructed. (Refer to figure 3.3.)

Thanks to the construction of LEDA, IPHI, and the TRASCO injector, high-intensity proton injectors can now be considered to be well-established devices. In all three cases, very good performances have been achieved, with beam specifications well above the EURISOL requirements. Consequently, we consider that these results fully demonstrate the feasibility of a 5-MeV, 5-mA CW proton injector (ion source plus room-temperature RFQ).

The fabrication cost of such an injector for the EURISOL proton driver accelerator is estimated to be somewhat lower than the cost of the IPHI project. Thus a cost of 10 M€ should be an upper limit for the EURISOL injector as a direct comparison with the present construction cost of IPHI (see table 3.2 below).

Table 3.2: IPHI components cost (M€).

SILHI source & LEBT	RFQ	Vacuum & diagnostics	RF & power supplies	Environment	Controls	TOTAL COST
0.6 M€	4.5 M€	1.1 M€	2.7 M€	0.8 M€	0.4 M€	**10.1 M€**

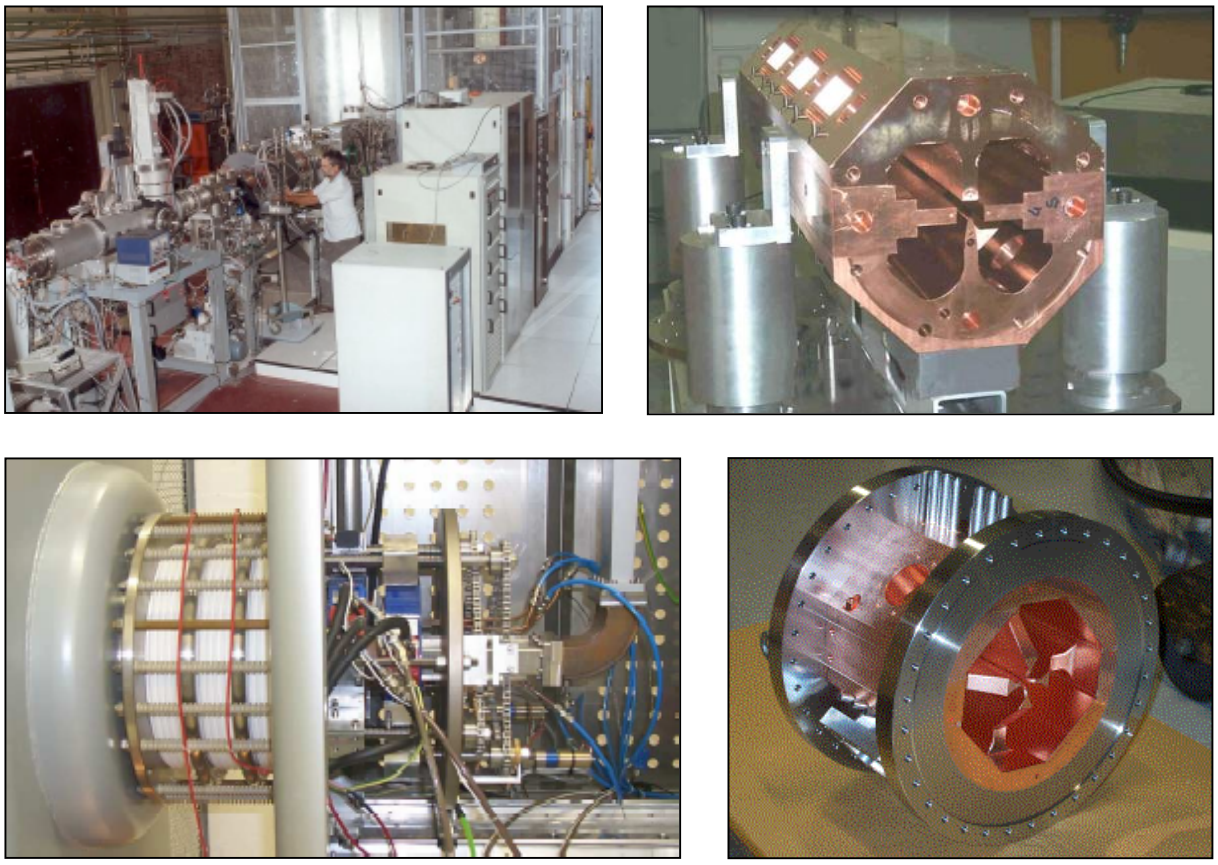

Fig. 3.3: (Top left:) The SILHI source and its test stand. (Top right:) The IPHI 352-MHz RFQ cold model. (Bottom left:) The TRIPS ion source on its 100 kV platform. (Bottom right:) Construction test of the TRASCO RFQ.

3.2 The intermediate-energy section (5–85 MeV)

We discuss here the linac between 5 and 85 MeV; for this range of energy, two main kinds of linac are operating at present: pulsed Drift-Tube Linacs (DTL), generally with a high proton peak current (at LANL, CERN, DESY, etc.), and superconducting low-current linacs (at ANL, LNL) for heavy ions. Moreover, high duty-cycle and CW DTLs are under construction (for SNS, IPHI) and superconducting linacs for this energy range are being studied for various applications.

We are therefore in the position to discuss both a warm and a cold solution, both with the same RFQ frequency (352 MHz). Owing to the large variation of the particle velocity in this part of the linac, the difficulties in the first (up to about 15 MeV) and second parts are somewhat different and the design choices often include two sub-sections. The specifications of the EURISOL intermediate section are indicated below.

Table 3.3: EURISOL intermediate section specifications.

Energy range	5–85	MeV
Beam current (CW)	5	mA
Beam loading	400	kW
Input transverse emittance	0.2π	mm.mr (rms normalised)
Input longitudinal emittance	0.2π	deg MeV (rms)
Frequency	352.2	MHz

3.2.1 Warm option

The structures developed or built for protons at this energy are mainly DTLs (Drift-Tube Linacs), SCDTLs (Side-Coupled DTLs) and CCDTLs (Coupled-Cavity DTLs).

The DTL is a structure that operates at the fundamental mode of a cylindrical structure; drift tubes are located every βλ-period. Quadrupole magnets are located inside each tube. In this case the RF power dissipation due to the capacitance between drift tubes can be high.

SCDTLs and CCDTLs both reach higher shunt impedance by using rather short cavities (with drift tubes every βλ) and keeping the quadrupoles outside the cavity. This means an increase in the transverse focusing period, which can in general only be done after some tens of MeV. SCDTLs and CCDTLs differ in the way the RF power is distributed between the cavities.

The existing machines and the designs developed in the last years are all either pulsed with high peak current or CW with high average current (30–100 mA). We have investigated what the situation could be for a comparatively 'low current' (5-mA) CW linac.

In table 3.4, we have extrapolated the main parameters of such a linac, starting from existing study designs optimised for different working currents.

In the first column we consider the SPL project of CERN, a pulsed linac for 11 mA peak current, 16.6 % duty cycle. The linac is composed of a DTL from 7 MeV up to 18 MeV, and a CCDTL up to 120 MeV. We considered the CW operation of this linac, a possibility that is briefly discussed in chapter 6 of the SPL proposal [26]. For our comparison we considered that the upgrade of the RFQ up to 7 MeV can be done without significant implications, and we stopped at 85 MeV.

In the second column we took the ASH project [27], where a CW 20-mA beam is considered. In this case a single kind of structure (DTL) has been adopted from 5 up to 85 MeV. The first part of this DTL is being constructed within the IPHI project. This second CW case is characterised by similar shunt impedance, and by a lower field so as to decrease the power dissipation density along the structure and to increase the efficiency.

Table 3.4: Extrapolations for a 5–85-MeV 5-mA CW warm linac.

Parameter	Extrapolated from SPL	Extrapolated from ASH	EURISOL proposal	Unit
Accelerating field	2.5	2	1.5	MV/m
Shunt impedance	20 – 50	35.5 average	35.5 average	MΩ/m
No. of tanks	66	13	-	-
Length	54	64	85	m
Beam loading	0.4	0.4	0.4	MW
Total RF power needed	5.8	5.4	4.4	MW
AC power (RF efficiency 50%)	11.6	10.8	8.8	MW
Efficiency	3.4	3.7	4.5	%
Approximate price	**-**	**25**	**20**	**M€**

For our application, we can decrease the field and the power dissipation even more (so as to increase the efficiency), which results in the values listed in the third column. Even accepting this longer linac, the RF power is much higher than the beam power (i.e. 4.4 MW, corresponding to 8.8 MW of AC power).

We have also looked at costs, starting from the cost estimates of SNS (25 M$), Concert (21 M$), ASH (25 M€) and SPL (22 M€); the 'EURISOL proposal' linac in the third column, if extrapolated from SPL, would cost 20 M€. What is important is that at this level of approximation all these prices are in the same range, which gives confidence in the value quoted.

3.2.2 Superconducting option

For several years, intensive studies have been done on SC cavities (e.g. spoke-type, quarter-wave resonators, re-entrant cavities, etc.) for their use as accelerating structures in the low-energy part of high-power proton or ion accelerators (typically from 5 to 100 MeV). In the following table, some characteristics of 3 kinds of resonators developed in Italy and France, and suited to our 352-MHz linac, are presented (see also figure 3.5).

Table 3.5: Characteristics of some SC resonators for the intermediate section.

Resonator type	QWR [ref. 28]	Re-entrant [ref. 29]	β=0.35 spoke [ref. 30]
Optimum beta	0.25	0.19 (nominal)	0.36
No. of gaps	2	1	2
Beam aperture (mm)	30	30	60
Peak surface electric field (MV/m)	33.6	25	25
Peak surface magnetic field (mT)	62	26	67
Voltage at nominal β per resonator (MV)	1.08	0.54	1.62
Real (physical) cavity length (mm)	180	80	354
Effective acceleration length (mm)	180	80	260
Real/effective accelerating gradient (MV/m)	6 / 6	6.8 / 6.8	4.6 / 6.2
Operating temperature (K)	4	4	2 or 4

The single-gap 're-entrant cavities' are modified pillbox cavities. A first prototype has been built for the TRASCO project [31] (see figure 3.5) and has been successfully tested at LNL, reaching the design field and Q without particular problems of multipacting [32]. The characteristics of such a cavity are wide velocity acceptance (single gap) and good field quality (no dipole, cylindrical symmetry). On the other hand, the energy gain per cavity is smaller that for two-gap cavities, and the number of cavities and complexity of the linac both increase. In the ADS context, this is justified by the high availability requirement, since in this way the beam survives the failure of one cavity. In the RIB context, these short structures, besides being the only ones so far demonstrated for this beta range, allow the design of a very flexible linac to accelerate ions other than just H^+.

The QWRs are simple to fabricate, and are currently being used in several heavy-ion accelerators, such as ALPI [33] at INFN-LNL operating at 80 MHz (see figure 3.4).

Fig. 3.4: Four low-beta quarter-wave resonators (80 MHz) assembled in the ALPI cryostat.

A 352-MHz version of such a QWR cavity has been developed at LNL (see table 3.5). Having two gaps, this cavity has a large velocity acceptance. For the EURISOL beam intensity, the effects of the electric and magnetic dipole fields can be overcome with a proper choice of lattice. A first prototype has been built (see figure 3.5) and will soon be tested. A construction using the same technique, but configured using half-wave resonators which have a convenient size at this frequency and are dipole free, is being explored at LNL and in other labs. Such cavities are very compact, though at the cost of slightly lower shunt impedance.

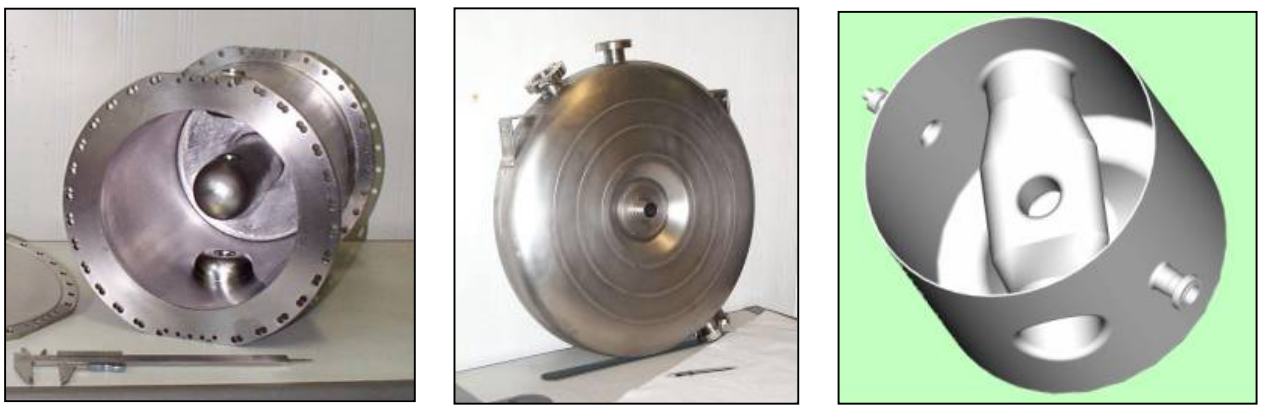

Fig. 3.5: Various types of resonator operated at 352 MHz; (left to right:) QWR, re-entrant and spoke-type.

Spoke-type cavities have been studied in recent years in various laboratories within the framework of several accelerator projects (AAA in Los Alamos for example [34]). The latest low-temperature tests performed on the prototype ANL (Argonne National Laboratory) spoke cavity have exhibited very good RF performance [35] (i.e. $E_{acc} > 12$ MeV/m and $Q_0 > 2 \times 10^9$ at 4 K). Some advantages of these cavities are their very low RF dissipation, good mechanical stability, their very small steering effect, and the possibility to have very large beam apertures. These characteristics are most promising and very interesting for building a highly reliable and safe accelerator, as is required, for example, in the ADS projects. An R&D program has started at IPN Orsay on this type of cavity, with the construction of a first β=0.35, 2-gap spoke prototype [36] that should be tested before end of 2002, and with some preliminary design studies on a β=0.15 2-gap spoke cryomodule [37].

The use of cavities with a larger number of gaps (i.e. 3 or 4), could give a simpler and more cost-effective linac, especially in the first part where the design of effective (even 2-gap) resonators seems difficult, and where the use of more gaps could reduce the number of cavities. A complete design of such cavities does not exist yet, but should be done in the R&D related to EURISOL, while a preliminary design can be found in refs [38] and [39]. For the high-energy part (above 20 MeV) also, the development of 4-gap cavities (simpler than at low energy) would allow an effective linac design, but one less suited to acceleration of heavy ions.

The linac structure is shown schematically in figure 3.6: 76 cavities (12 4-gap and 64 QWR or HWR cavities) and 54 superconducting quadrupoles are housed in 10 cryostats, for a total length of approximately 45 meters. There are four families of cavities, with optimum β=0.12, 0.17, 0.25 and 0.33, respectively, and with the corresponding four kinds of cryostats. The four types of cavities operate at the same accelerating field (6 MV/m) and have similar beam loading per cavity (see figure 3.7). The use of solid-state RF amplifiers is foreseen. A high-efficiency, 2.5-kW prototype unit has been built at LNL [40]. The amplifier construction is modular and units of 2.5, 5, 7.5 and 10 kW can be built at relatively low cost and with compact size. The superconducting quadrupole used in this design has been prototyped at MSU for application in the TRASCO ISCL [41].

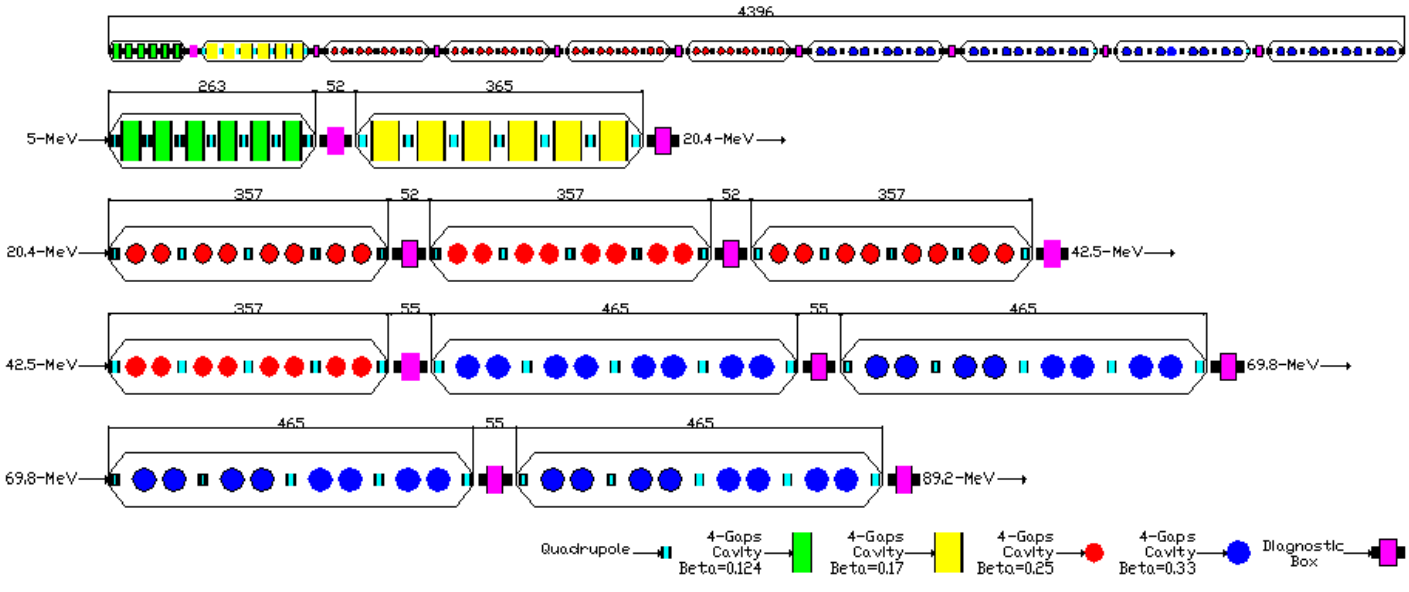

Fig. 3.6: Schematic layout of the linac using 4-gap cavities and QWRs or HWRs.

The basic focusing structure is a FODO, with a constant period length in each cryostat. The period length increases with each successive type of cryostat, since the cavities themselves become longer. A diagnostics box is located at each warm transition, for a total of 9 positions. Beam envelopes and beam rms dimensions corresponding to 5 mA of current are plotted in figure 3.7. This preliminary simulation was performed with PARMILA using 100 000 macro-particles. The residual mismatch due to the transitions can be seen, but the maximum beam dimensions are well below the bore radius. The emittance increase is negligible. The bore is well above 7 times the rms radius, all along the linac. This figure takes into account the different bore radius in cavities and quadrupoles shows one of the main advantages of ISCLs over DTLs. The ratio is in general smaller in the quadrupoles, where we prefer to have any possible losses.

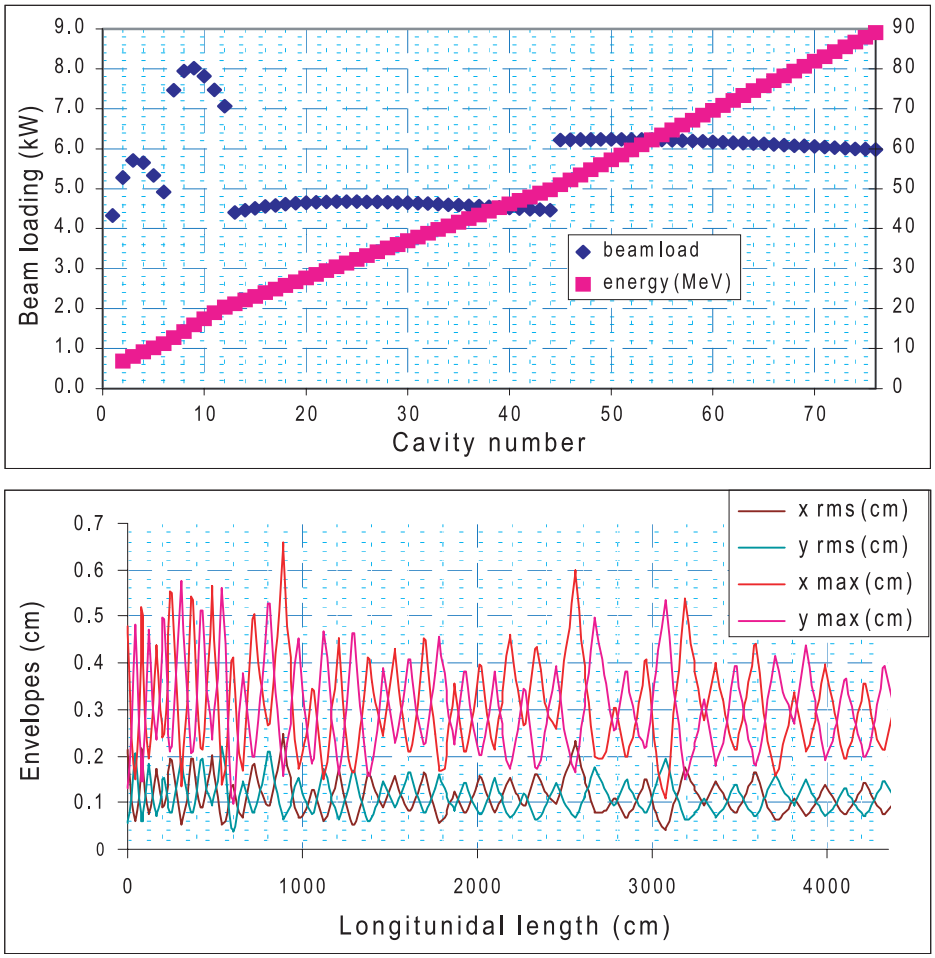

Fig. 3.7: (Top:) Beam loading and beam energy. (Bottom:) Beam envelopes in the (4-gap + QWR or HWR) linac.

The space-charge effect is not dominant (initial transverse tune depression is about 10%) and the same beam matching can be used to transport up to more than 50 mA of beam current with full transmission. The results of various runs with different beam intensities show that this linac, optimised for 5 mA where the emittance growth is practically zero, maintains – with the same settings – an acceptable emittance growth up to 10 mA (about 20%). A lower emittance can be obtained with new beam matching, if necessary.

In a second (independent) design inspired by the IPN Orsay study mentioned earlier, 2-gap spoke cavities with very large beam aperture (6-cm diameter instead of 3 cm) have been used. These SC cavities are grouped in cryomodules containing superconducting focusing devices (quadrupole

doublets). Longitudinal beam dynamics calculations show that two beta values are enough to cover the whole energy range (5–85 MeV): 30 β=0.15 (geometrical beta) cavities are used for the 5–18 MeV section (1 cavity per focusing lattice), and 58 β=0.35 cavities for the 18–85 MeV section (2 cavities per focusing lattice). The choice of the linac architecture has been made keeping large margins, so as to ensure both a reliable operation of the acceleration structures and of RF components, and a very high robustness of the focusing design [42]. This results in quite a long linac (95 m), but this may be the price one has to pay for the increased reliability, which then provides for a highly fault-tolerant focusing design, in which the failure of most of the components could be allowed.

For this section and for the high-energy section (see section 3.3.2), beam dynamics simulations have been performed with TraceWin and Partran. In these calculations, the IPHI RFQ exit beam distribution was used as the input beam for the spoke linac, and the matching between the RFQ and the spoke linac was achieved by simply adding another β=0.15 spoke module, in which the 2-spoke cavities are used as bunchers. Simulation results show very smooth envelopes (see figure 3.8), and an emittance growth below 5%. Note that some preliminary simulations also indicate that this design should be quite fault-tolerant, both in the case of mismatched beams, and in the case of failure of a component (whether a cavity or a quadrupole).

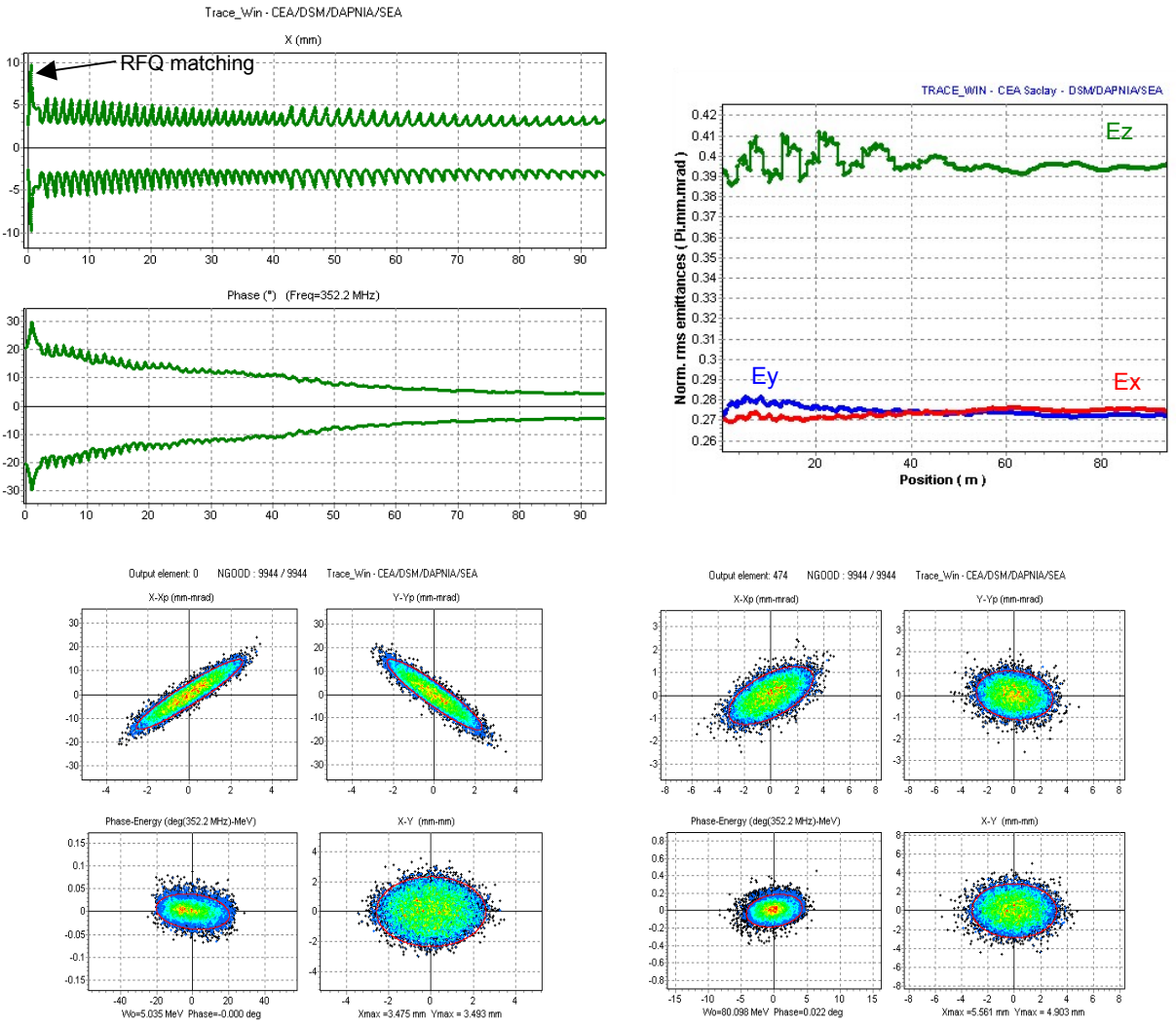

Fig. 3.8: Beam tracked through the linac (matched case) up to 80 MeV (10 mA beam). (Top left:) 100% envelopes. (Top right:) RMS emittance evolutions (multi-particle calculations). (Bottom left:) Beam distributions at the RFQ output (5 MeV). (Bottom right:) Beam distributions at the spoke linac output (80 MeV).

The main characteristics of the two proposals, which are very similar in the efficiency and the total number of cavities, are presented in the following table. In each case, the cavities are fed by independent RF power supplies for flexibility and reliability. The main difference is the total length of the linac, which is quite short in the QWR case, mainly owing to the use of very compact cryomodules (these are also more expensive, however – see tables 3.8 & 3.9), but also because of the very comfortable margins used in the spoke linac focusing design to obtain a highly reliable machine. An estimate of the heat loads is also given for the solution combining both 4-gap cavities and QWRs (see table 3.7).

Table 3.6: Characteristics of the two proposed 5–85 MeV linacs.

Linac type:	4-gap + QWR	2-gap spoke
Total number of cavities	76	88
Length (m)	45	95
RF beam power (kW)	400	400
RF auxiliary power (kW)	100	100
Heat load (W)	1200 @ 4K	200 @ 2K
AC power for RF (kW)	1000	1000
AC power for cryogenics (kW)	300	300
Efficiency (%)	38.5	38.5

Table 3.7: Heat loads at 4.5 K for the 4-gap + QWR 5–85-MeV linac.

Heat Load	Unit consumption.	No. of units	Total
Dissipated in each cavity	10 W	76	760 W
Static losses per metre of length	10 W	45	450 W
Total @ 4.5 K:			**1210 W**

Finally, a first cost estimate is given in table 3.8, giving a construction cost of **22.1 M€** for such a 5–85 MeV proton accelerator (4-gap + QWR proposal). An independent cost estimate has also been done for the second option (using 2-gap spoke cavities) with a total cost of **23.1 M€** (see table 3.9) Moreover, the option using 28 re-entrant cavities up to 17 MeV (instead of the 13 4-gap cavities) leads to a price of **24.1 M€**. All these versions are in the same order of price, and can cope with acceleration of $A/q = 2$ ions (see section 4).

3.2.3 Comparison between warm and cold options

The investment cost for both warm and cold options seems to be of the same order. The length of the linac, which is also the same order of magnitude for both the superconducting and the DTL options (between 55 & 95 metres), is not a relevant issue.

On the other hand, we stress that the AC power difference is large (8.8 MW compared with less than 1.5 MW) and makes a big difference in the operating cost – of the order of 2 M€ per year.

Table 3.8: Estimated costs for the 4-gap, QWR, 5–85-MeV linac.

Component	Unit price	No Units	Total
4-gap cavity construction (each)	150 k€	12	1.8 M€
QWR cavity construction (each)	60 k€	64	3.84 M€
Coupler (each)	15 k€	76	1.14 M€
Cryostat (per metre of length)	100 k€	45	4.5 M€
Quadrupoles (each)	20 k€	54	1.08 M€
RF (7.5 kW, solid state)	45 k€	76	3.42 M€
Controls (5%)	-	-	0.9 M€
Vacuum	-	-	0.25 M€
Diagnostics	-	-	1.0 M€
Cryogenics (2 kW @ 4.5K)	-	-	4.2 M€
TOTAL:	-	-	**22.1 M€**

Table 3.9: Estimated costs for the (2-gap spoke) 5–85-MeV linac.

Component	Unit price	Total
Niobium (per cavity)	15 k€	1.3 M€
Cavity fabrication with tuner & tank (each)	50 k€	4.4 M€
Coupler (each)	25 k€	2.2 M€
Q-poles doublets (each)	40 k€	2.4 M€
RF (IOT) + power supplies (each)	80 k€	7.0 M€
Vacuum (per cavity)	5 k€	0.45 M€
Diagnostic (per cavity)	5 k€	0.45 M€
Cryostat (per metre of length)	20 k€	1.6 M€
Cryogenic system (300 W @2K)	-	2.3 M€
Controls	-	1.0 M€
TOTAL:	-	**23.1 M€**

Note that the cooling system necessary for the warm solution is not included in the cost estimate, while the cryogenic power needed for the cold solution is considered part of the capacity of the main refrigeration plant.

Two interesting features of the superconducting solutions are the larger beam aperture (higher safety) and the possibility of independent control of the phases. This second characteristic would allow acceleration of ions with charge-to-mass ratio of 1/2, and for the re-entrant cavity option 1/3, up to about the same maximum energy per charge.

Finally, we feel that the second part (from 17 or 18 MeV to 85 MeV) of this section can be conveniently done with different kinds of SC cavity, with the great advantage of non-negligible savings on the operating cost; on the other hand, the first part (5–17 MeV) has to be longitudinally very compact, which makes the design more difficult. More R&D is needed at this point, and a back-up solution for this part can be a warm DTL, such as the low-energy section soon to be tested within the IPHI project.

3.3 The high-energy section (85 MeV to 1 or 2 GeV)

The proposed superconducting linac for the 'high-energy' section of the proton EURISOL driver is based on an original study from the ASH (France) and TRASCO (Italy) projects, which lead to a common design for an ADS driver (a collaboration between the CEA-CNRS in France, and the INFN in Italy) [43]. One major initial proposal of this collaboration was to adopt elliptical superconducting cavities operating at a frequency of 700 MHz, to take advantage of the successful technological progress made by the TESLA project [44] with its multi-cell niobium cavities: by applying the well-established fabrication and preparation techniques, high accelerating gradients can now be reached in low-β cavities.

During the last two years, the French-Italian collaboration has concentrated its efforts in setting and developing optimisation criteria for the cavities and the linac design. In parallel, an R&D program was started in both countries, with the construction and test of the first single-cell prototypes (β=0.47 and 0.65). Four of the best results obtained during this period are presented in the figures below. Accelerating gradients of more than 25 MV/m were reached in two β=0.65 cavities, exceeding by far the design goal, while very good results were also demonstrated in the first low-quality niobium β=0.47 prototypes. [Note that the multipacting barriers encountered here disappear after RF processing].

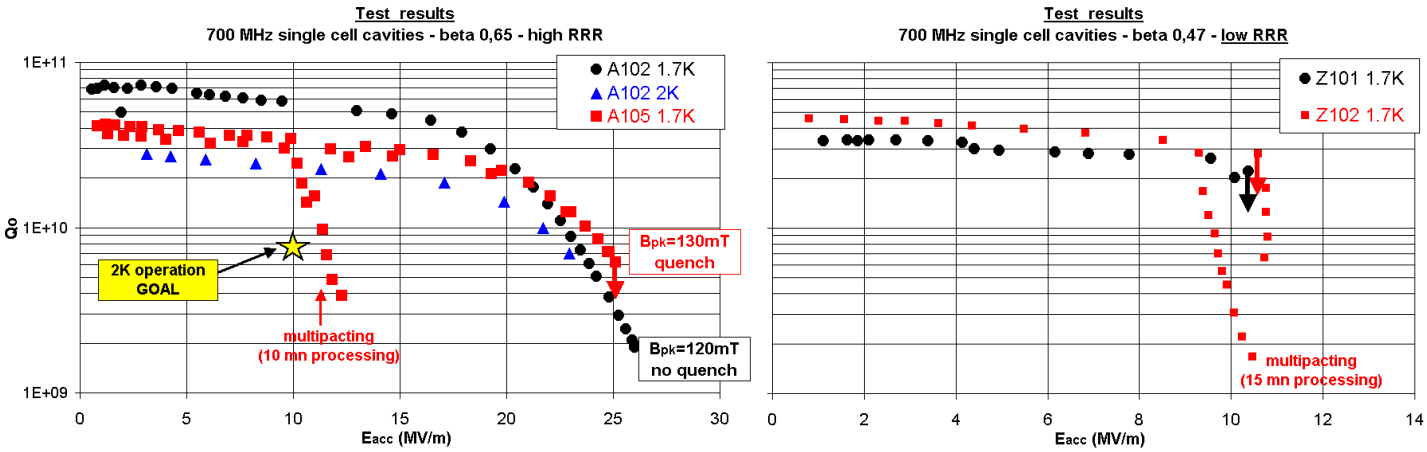

Fig. 3.9: Test results for 700-MHz single-cell cavities fabricated for the CEA-CNRS-INFN collaboration.

The APT-AAA project at Los Alamos has also chosen the 700 MHz frequency with the same TESLA technology. Four multi-cell cavities (5 cells, β=0.65) were fabricated by CERCA in France in 2000, and the tests showed encouraging results: gradients in the range of 9–11 MV/m were obtained [45], exceeding by a factor of two the required performance. Other high-intensity linac projects have also chosen superconducting cavities for their design, but at different frequencies: SNS (USA) at 805 MHz [46], SPL (CERN) at 350 MHz [47] and KEK-JAERI (Japan) at 600 MHz [48]. The SNS project is now entering the construction period with a very

active fabrication and test phase; the first 6-cell prototypes showed excellent results with accelerating gradients reaching 16 MV/m for the β=0.61 cavity and 19 MV/m for β=0.81 [49]. The other two projects also have intense R&D programmes with both prototypes and design studies. All this will contribute to a very rich and creative period that should produce significant improvements in this technology.

Finally, all the studies started in many countries are converging towards the use of superconducting cavity technology in the high-energy section of this kind of linear proton accelerator. This choice has many significant advantages compared with the classical room-temperature solution: very high power efficiency (savings on operation and investment costs), high gradients (much shortened linacs), safety (large beam apertures), flexibility, etc. In the following paragraphs, a detailed presentation of the first studies for the superconducting high-energy section of the EURISOL proton linac is presented.

Discussion is given on the choice of cavity geometry, focusing scheme, cavity grouping within cryomodules, beam dynamics, the RF system, cryogenics, safety aspects and the overall layout of the linac. A short presentation of the proposed R&D program, and a first cost estimate are also presented.

In optimising the EURISOL high-energy section (5 MeV to 1 or 2 GeV, 5 mA CW), the main goals are to:

- ***maximise the accelerating fields keeping the peak surface fields in the cavities below fairly conservative values (50 mT for B_{pk} and 30 MV/m for E_{pk});***
- ***minimise the RF losses;***
- ***minimise the linac length;***
- ***minimise the number of sections to reduce the cavity development effort;***
- ***provide acceptable beam dynamics (quite easy for only a 5-mA beam).***

A preliminary study based on these features leads to the following basic choices:

- **an operating frequency of 704.4 MHz;**
- **an operating temperature of 2 K;**
- **5-cell cavities (a good compromise between linac length and energy acceptance);**
- **3 different sections to cover the energy range 85 MeV to 1 or 2 GeV, with β=0.47, β=0.65 & β=0.85 cavities.**

3.3.1 Cavity design.

The EURISOL cavity design is derived from the study made for the ASH/TRASCO project (CEA/INFN/IN2P3 collaboration) [50]. The RF calculations were performed with Superfish and BuildCav [51]; the mechanical simulations were done using Castem and Ansys. The main goals of the optimisation study were:

- ***Minimisation of peak surface fields ratio E_{pk}/E_{acc} and B_{pk}/E_{acc}.***
- ***Minimisation of dissipations on the cavity walls.***
- ***Large beam holes (>20 × rms beam size) + inter-cell coupling >1%.***
- ***Acceptable mechanical stability (mechanical stress kept below 50 MPa below 2 bars external pressure; note that Lorentz-force detuning is not a crucial issue for this CW linac).***

The optimised geometrical parameters of the EURISOL cavities are presented in table 3.11. A view of the β=0.65 cavity is also given (from SUPERFISH) in figure 3.10. Note that the right external cell has a larger bore so as to couple the RF power to the beam more easily (since Q_{ext} of the order of some 10^6 is needed). Mechanical simulations show that these cavities have good mechanical properties (see figure 3.10): an additional stiffening is only needed for the β=0.47 cavity due to its very steep walls. Note that for use with a pulsed beam, additional stiffening should be added for all cavities so as to keep the Lorentz detuning coefficient below a few Hz/(MV/m)². Finally, the unloaded Q-values at 2K are expected to be well above 10^{10} in this kind of cavities. The accelerating field (see figure 3.11) should exceed 8, 10 and 12 MV/m, respectively, in the 3 different sections of the linac, while keeping the peak magnetic surface field under 50 mT. The main RF characteristics of the EURISOL cavities are presented in the table below.

Table 3.10: Main RF characteristics of the EURISOL elliptical cavities.

At $\beta=\beta_g$ (geometrical β)	β_g=0.47 cavity	β_g=0.65 cavity	β_g=0.85 cavity
B_{pk}/E_{acc} (mT/MV/m)	5.88	4.88	4.07
E_{pk}/E_{acc}	3.58	2.61	2.37
r/Q (Ω) circuit definition	79.5	157.5	248.2
G (Ω)	158	199	263
K (%)	1.35	1.11	1.17

Table 3.11: Geometrical parameters of the EURISOL elliptical cavities. (Refer to figure 3.10)

Dimension	β_g=0.47 cavity			β_g=0.65 cavity			β_g=0.85 cavity		
(refer to fig 3.10)	left external cell	internal cell	right external cell	left external cell	internal cell	right external cell	left external cell	internal cell	right external cell
Cell length L (cm)	10	10	10	14	14	14	18	18	18
Full radius R (cm)	18.7	18.7	18.7	18.64	18.64	18.64	18,62	18.62	18.62
Iris radius R_b (cm)	4	4	6.5	4.5	4.5	6.5	5.0	5.0	6.5
Wall angle α (°)	5.98	5.5	4.84	8.85	8.5	5.6	9.1	8.5	5.74
Wall position d (cm)	0.7	0.7	0.6	1	1	1	1	1	0.8
b (cm)	1.04	1.03	0.87	1.59	1.58	1.48	1.75	1.72	1.29
a (cm)	0.8	0.79	0.67	1.22	1.21	1.14	1.25	1.23	0.92
B (cm)	5.6	5.38	3.66	4.96	4.51	5.3	7.63	6.92	7.72
A (cm)	3.3	3.36	3.66	4.51	4.51	5.3	6.93	6.92	7.72
Full length (cm)	85			105			125		
Niobium thickness (mm)	4 (stiffening needed)			4 (no stiffening)			3 (no stiffening)		

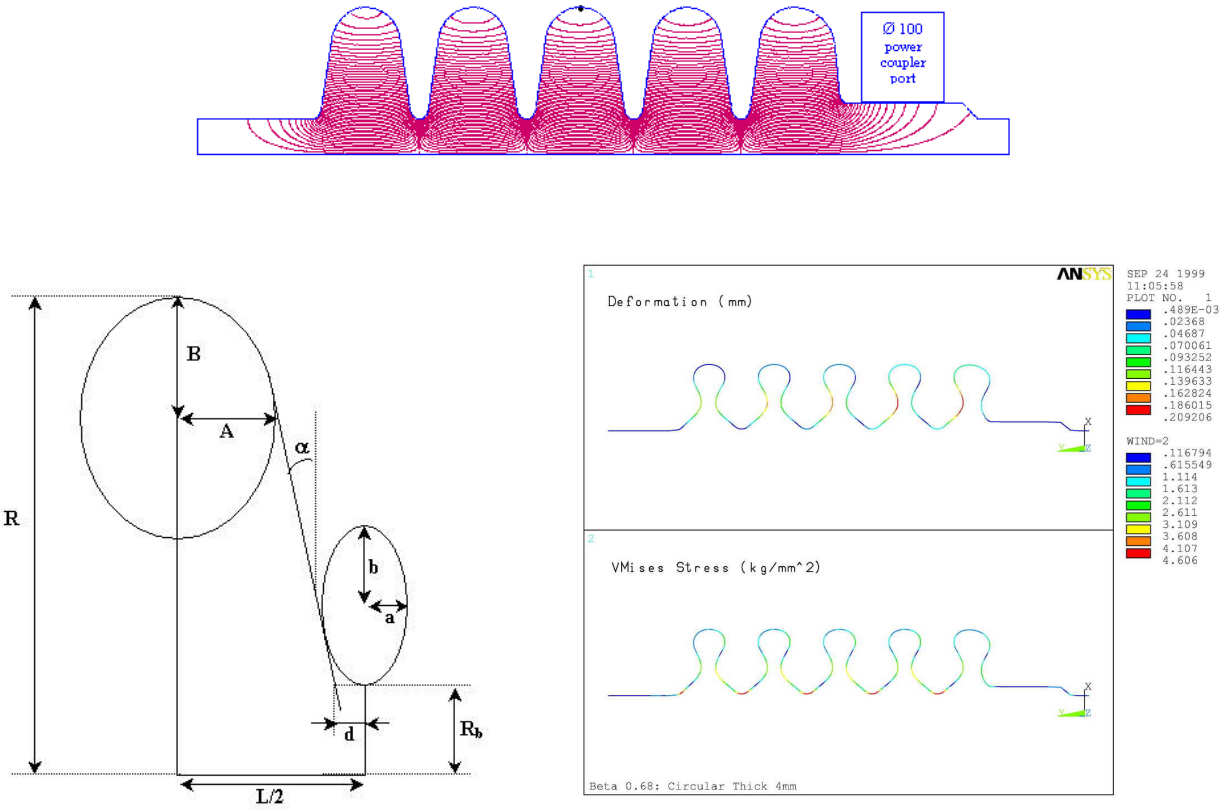

Fig. 3.10: (Top:) RF calculations for the β=0.65 cavity with SUPERFISH. (Bottom left:) Half-cell geometrical parameters. (Bottom right:) Mechanical calculations for the β=0.65 cavity with ANSYS (for a 2-bar external pressure).

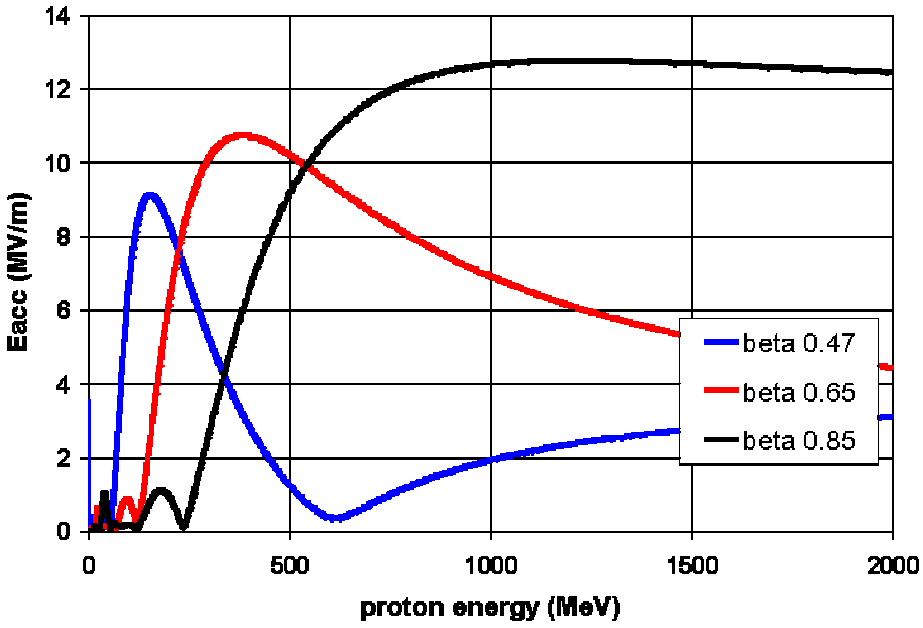

Fig. 3.11: Accelerating field in the high-energy section (normalised for B_{pk}=50 mT).

3.3.2 Focusing design

The EURISOL preliminary focusing design is derived from the existing beam dynamics studies already done in the field of high-power proton accelerators. The specific calculations performed in the frame of the EURISOL project are based on:

- the use of room-temperature quadrupole doublets inserted between cryomodules (gradients are kept below 10 T/m);
- smooth growth of focusing period length (4.1 m, 5.65 m & 8.1 m respectively in the 3 sections);
- synchronous phase chosen around –25° to provide good longitudinal focusing while maintaining efficient acceleration;
- minimisation of the emittance growth – and of the sensitivity to beam mismatch, current variation, misalignment and field errors – by keeping the evolution of the zero-current phase advance per metre as smooth as possible, while staying below 90° per focusing lattice to avoid beam instabilities (figures 3.12);
- matching between sections by maintaining equal values of the longitudinal and transverse zero-current phase advance per meter at each side of the transition (synchronous phase and quadrupole gradients slightly adjusted);
- equipartitioning factor (k_{0l}/k_{0t}) everywhere below unity, to avoid collective beam resonances between longitudinal and transverse planes.

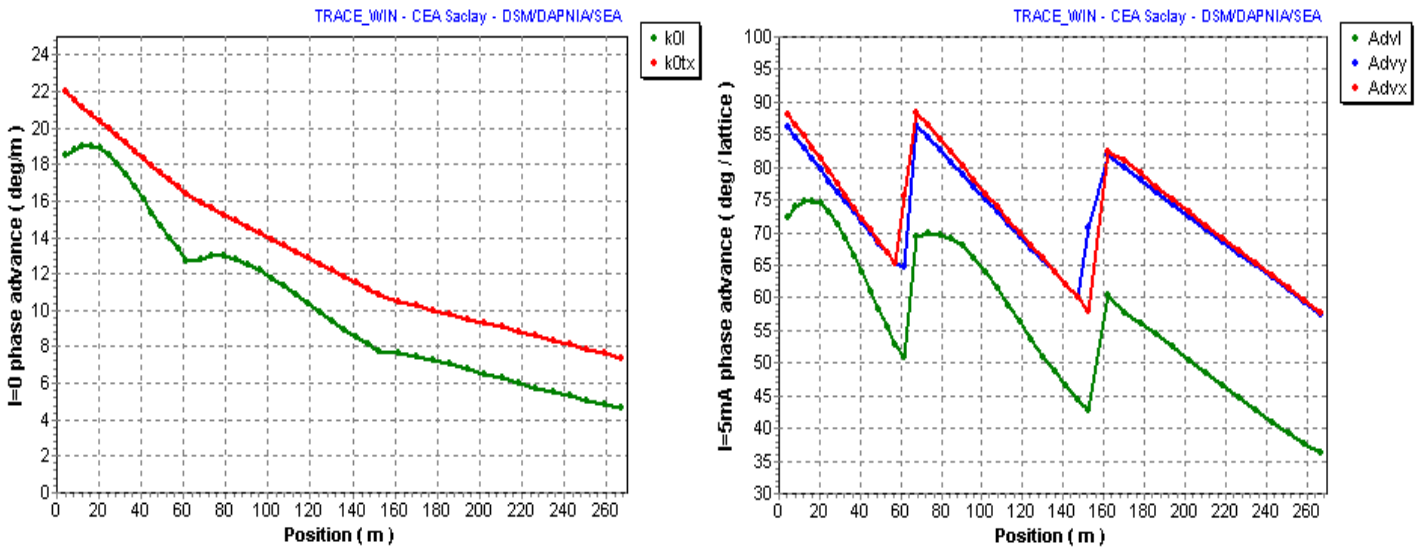

Fig. 3.12: Evolution of phase advance up to 1 GeV. (Left:) Zero current, deg/metre. (Right:) 5 mA, deg/lattice).

Beam dynamical calculations were performed using codes GenLin and TraceWin (developed at CEA Saclay by N. Pichoff and D. Uriot) for envelope calculations, and Partran with the PicNic space-charge routine for multi-particle calculations (with 100 000 particles). The beam specifications chosen at the entrance of the high-energy section (85 MeV) are the following: $\varepsilon_x=\varepsilon_y=0.25\pi$ mm.mr (normalised rms), $\varepsilon_z=0.45\pi$ mm.mr (normalised rms), 5-mA beam. The transition from the linac's intermediate part (<85 MeV) was not precisely studied; however, that the transition should be easier to match with a superconducting section than with a warm DTL.

The envelopes obtained are very regular (see figure 3.13), showing a very good matching between the different sections. There is no emittance growth in any of the three planes, either for the rms or for the 99% emittances, and the beam distribution does not exhibit any halo (figure 3.15). The rms beam radius at the high-energy end (1 GeV) is about 1.4 mm (less than 35 times the bore radius), and the 100% beam radius is about 3.5 mm, giving a significant safety margin for halo particles.

To test the stability of the optics design, a strongly mismatched input beam was tracked (30% mismatch in the three planes). Both rms and 99% emittance growths stay below a few percent in each of the 3 planes (figures 3.14 & 3.15). The rms beam radius at the high-energy end stays below 2 mm, giving us much confidence in the safety of our design. Note that all these calculations were done in an 'error-free' linac (with no misalignments, no gradient errors, etc.).

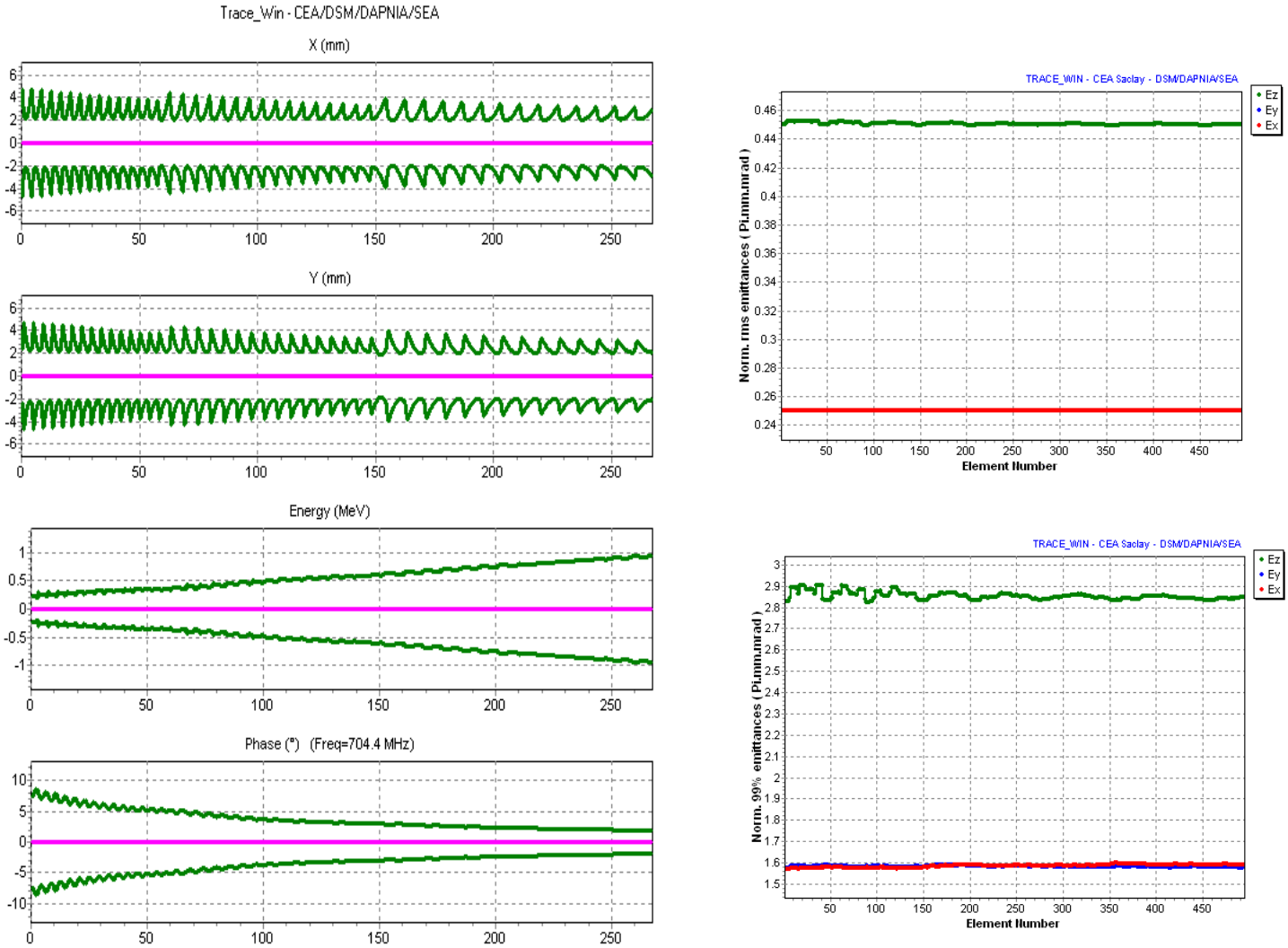

Fig. 3.13: Beam tracked through the linac (matched case) up to 1 GeV. (Left:) 100% envelopes. (Right:) RMS & 99% emittance evolutions (multi-particle calculations).

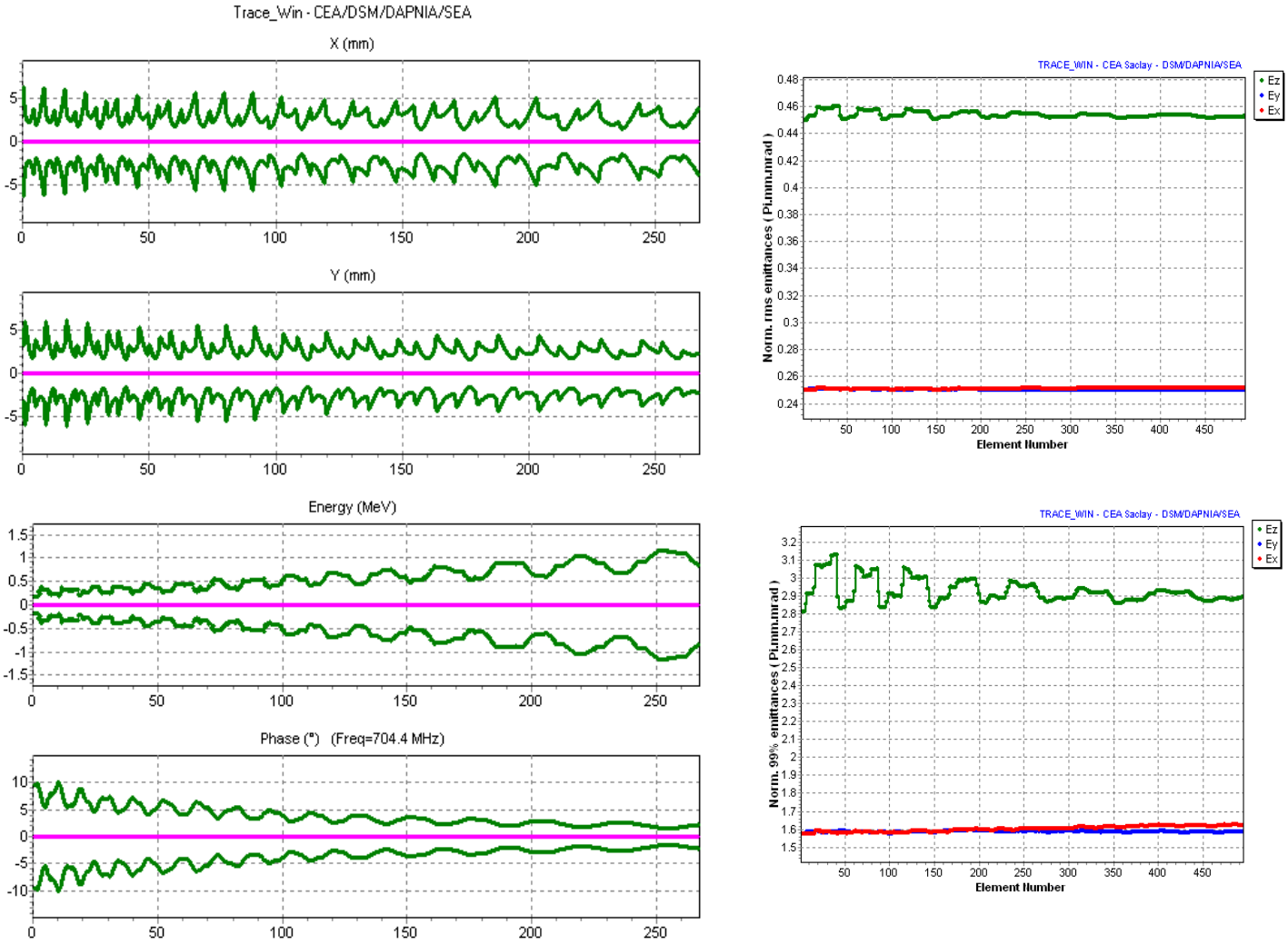

Fig. 3.14: Beam tracked through the linac (mismatched case) up to 1 GeV. (Left:) 100% envelopes. (Right:) RMS & 99% emittance evolutions (multi-particle calculations).

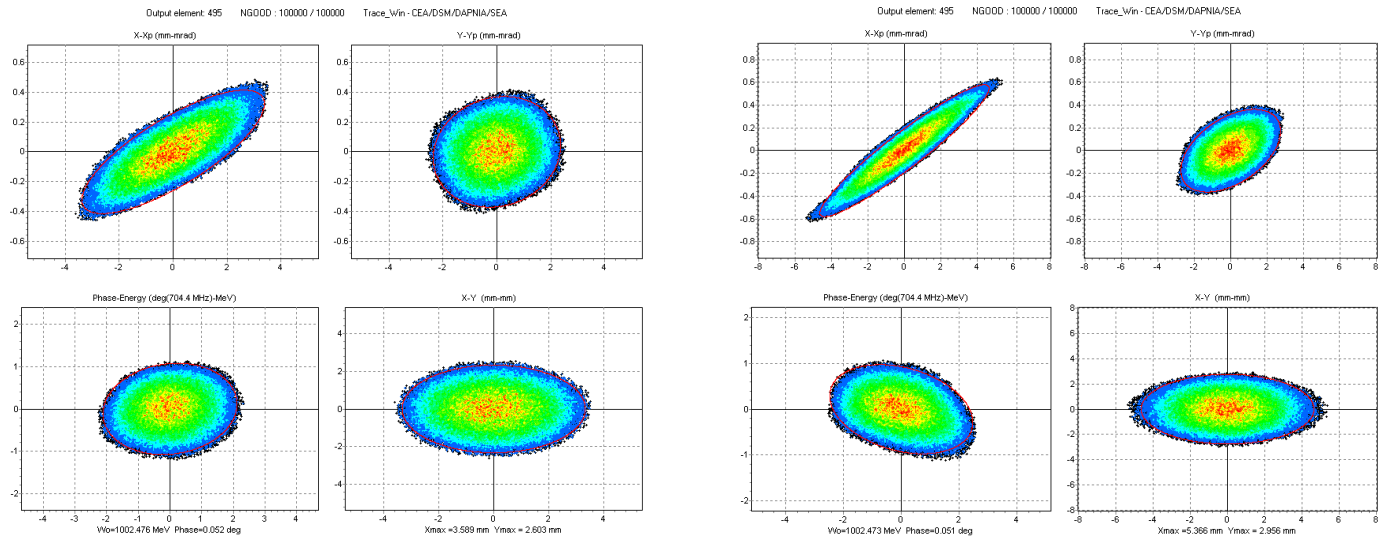

Fig. 3.15: Beam distributions from Partran at the high-energy end (1 GeV). (Left:) Matched case. (Right:) Mismatched case.

3.3.3 General linac layout

The main parameters and results for the EURISOL 85-MeV – 1-GeV, 5-mA linac (~270 m long) are contained in the following table and figures. Note that for a 2-GeV linac, 39 modules instead of 14 are needed in the β=0.85 section. The layout of the cryostats is given on the next page.

Table 3.12: Main characteristics of the EURISOL high-energy section (up to 1 GeV).

Parameter	β=0.47 section	β=0.65 section	β=0.85 section
Input energy (MeV)	85	192	481
No. of cavities per module	2	3	4
Lattice length (m)	4.1	5.65	8.1
No. of modules	15	16	14
No. of cavities	30	48	56
Section length (m)	61.5	90.4	113.4
E_{acc} (MV/m)	4.6 to 9.1	5.7 to 10.7	8.8 to 12.6
Synchronous phase (°)	-25	-25	-25
Real gradient (MeV/m)	1.1 to 2.0	2.0 to 3.6	3.6 to 5.1
Maximum E_{pk} (MV/m)	30	27	29
Maximum B_{pk} (mT)	50	50	50
RF power/cavity (kW)	10.5 to 20.7	17.5 to 34.1	36.1 to 51.7
Total dynamic cavity losses @ 2K (kW) $Q_o=10^{10}$	0.35	0.79	1.38
Quadrupole length (cm)	25	25	50
Quadrupole gradient (T/m)	6.1 to 7.8	8.0 to 10.0	4.6 to 5.4
Aperture radius (mm)	40	45	50
Ratio of aperture radius to max. rms beam size	19	23	28

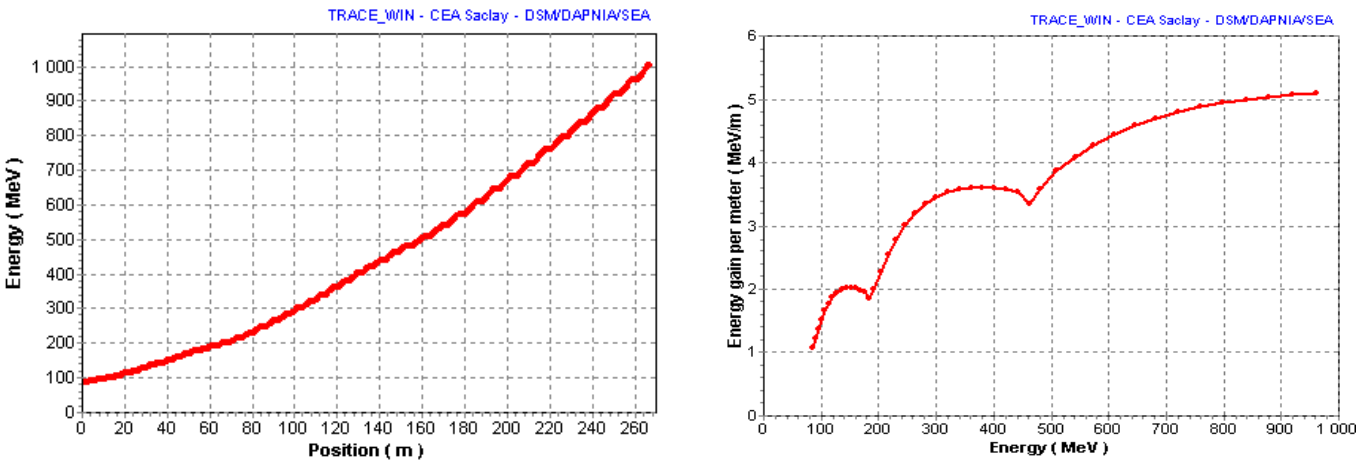

Fig. 3.16: (Left:) Energy evolution along the linac. (Right:) Energy gain per real metre (i.e. real gradient).

β=0.47 section: 85 MeV – 192 MeV:

- Total length = 61.5 m, lattice length = 4.1 m, cryomodule length = 2.8 m.
- 15 modules, 2 cavities per cryomodule.

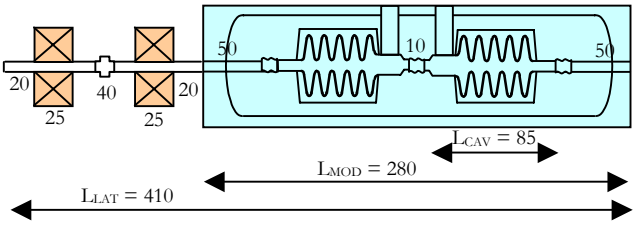

β=0.65 section: 192 MeV – 481 MeV:

- Total length = 90.4 m, lattice length = 5.65 m, cryomodule length = 4.35 m.
- 16 modules, 3 cavities per cryomodule.

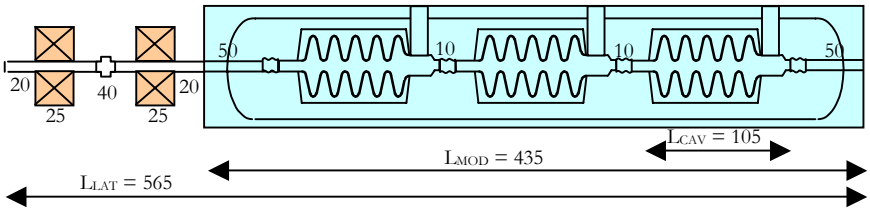

β=0.85 section: 481 MeV – 1 GeV (2 GeV):

- Total length = 113.4m *(315.9 m)*, lattice length = 8.1 m, cryomodule length = 6.3 m.
- 14 modules *(39 for 2 GeV)*, 4 cavities per cryomodule.

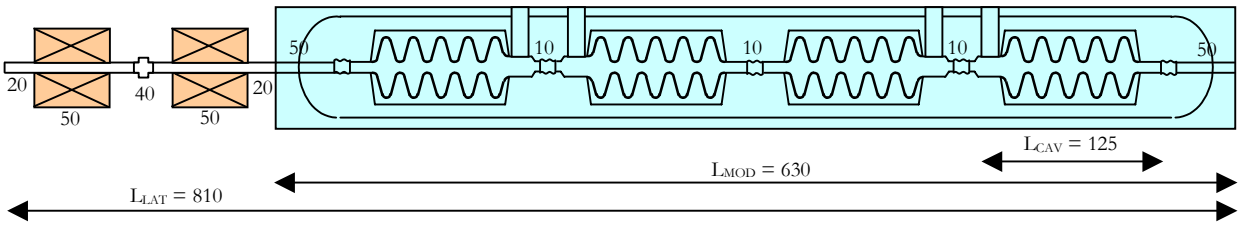

Key to diagrams above:

Quadrupole .....

Cavity + power coupler .....

Bellows .....

Valve, diagnostic element .....

(Note: all distances given in cm.)

3.3.4 RF system

The curve in the figure below gives the power needed in each cavity for CW operation at nominal current (5 mA) for a 1-GeV linac.

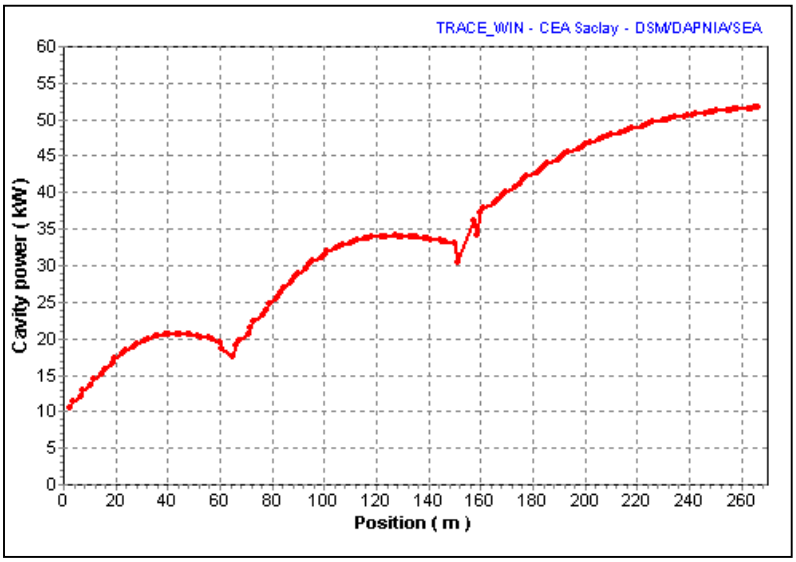

Fig. 3.17: RF power needed per cavity along the 1-GeV linac.

It is proposed that each cavity be driven with an independent RF power source in order to obtain precise control of each cavity's accelerating gradient and phase. This is an important design aspect closely related to the fine matching of the different sections, and in general to the improvement of the accelerator reliability.

These power levels, in the range 10 kW to 52 kW, can easily be reached with commercial IOT tubes (EEV, Thomson). In recent tests, a Thomson IOT tube (ref. no. 790) exhibited power levels reaching 80 kW with very good efficiency (>65%). This model could perfectly fit the needs in the high-energy range; lower-power models (40 kW) could eventually be more interesting for the low-energy range. Note that the power converters (AC-DC) could be grouped in units of 250 kVA or 500 kVA, as indicated schematically in figure 3.18.

Table 3.13: Power needs of the RF system for the 85-MeV – 1-GeV section.

Type of cavity	Number of cavities	RF Power needed (kW)
β = 0.47	30	535
β = 0.65	48	1 445
β = 0.85	56	2 595
Total (85 MeV 1 GeV)	**134**	**4 575**
Total DC power (efficiency ~ 60 % on average)		7625
Total AC power (~ 90 % efficiency)		**8470**

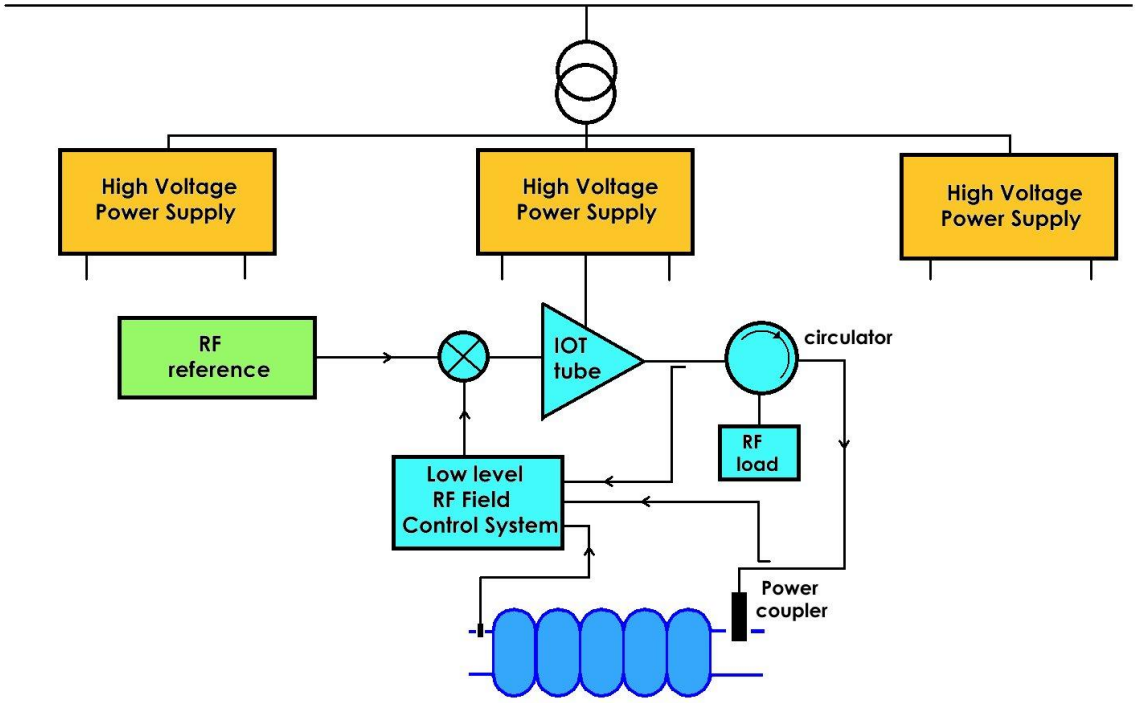

Fig. 3.18: General scheme of the RF system.

3.3.5 Cryogenic system

The operation of SC cavities at 2K is an interesting choice since the dynamic losses – directly proportional to the RF surface resistance – are drastically reduced. In a first approach, this resistance is reduced by a factor greater than 10 compared with a 4.2K operational temperature. The gain obtained in thermal stability by increasing both the quench margin and the high heat transfer capability of superfluid helium is also a favourable condition.

On the other hand, the cryogenic system is more complicated, needing the introduction of low-temperature compressors operating at low pressures, reducing the overall thermodynamical efficiency. Nevertheless, several large facilities such as CEBAF are now in routine operation with good reliability. Moreover, the technical progress related to the future LHC makes us quite optimistic about this choice.

The following table summarises the heat loads for the 45 cryomodules needed in the EURISOL high-energy section (up to 1 GeV).

Table 3.14: Main RF characteristics of the EURISOL elliptical cavities.

Temperature level	Dynamic losses	Static losses	Total
2K [(a)]	2 700 W	660 W	3 360 W
4.5K [(b)]	1 020 W	2 680 W	3 700 W (4.9 g/s)
Thermal shields (~ 50K)[(c)]	-	4 300 W	4 300 W

(a) Losses in the cavities and associated cryogenic circuits in the cryomodules.

(b) Losses in the power-coupler cooling loops.

(c) Losses in cryomodule thermal shields. The temperature can range between 35K and 75K (to be optimised).

If we assume an efficiency of 1.5×10^{-3} (thermodynamic and technical efficiency) for the 2K temperature level, 4×10^{-3} for the 4.5K level, and 5×10^{-2} for the 50K level, the total AC power consumption of the refrigerator operating at nominal beam conditions will be about 3.2 MW. The overall beam efficiency can be roughly estimated as follows:

$$\begin{aligned}\text{Beam efficiency} &= (\text{beam power})/(\text{RF} + \text{cryo-power}) \\ &= 5\ \text{MW}/(7.83 + 3.2)\ \text{MW} \\ &\approx 45\%\end{aligned}$$

Finally, the 1-GeV high-energy section will require a refrigerator with the following capacities (including a safety margin of 30%):

- **350 W @ 2K**
- **800 W (6.5 g/s) @ 4.5K**
- **600 W @ 50K**

The size of this refrigerator is close to that of the CEBAF facility. This system, after several years of reliable operation, is now running very stably, delivering more than 5 000 hours of beam to the experimental areas each year. In more recent projects, like SNS and TESLA, the proposed refrigeration cycles and the conceptual technical layout are also similar to the CEBAF system.

3.3.6 Safety aspects

An essential requirement of this linac design is to keep beam losses to below the standard 1 W/m level. The main mechanism resulting in beam loss in a proton linac is the beam halo formation and its impact with the vacuum chamber. The preliminary calculations with 100 000 particles presented in a previous section showed that we can be quite confident in the safety of our linac design, since even with a strongly mismatched input beam, the ratio between the minimum aperture radius and the maximum beam radius remains very high, leaving significant safety margins against an unforeseen increase of beam radius.

These safety margins are of the same order of magnitude as those chosen by different projects like the SNS, the SPL or the CONCERT projects; moreover, the EURISOL linac has inherent advantages for the safety point of view:

- the beam is not pulsed, which decreases the risk of longitudinal beam losses due to phase and amplitude errors in RF cavities.
- the bunch current is very low compared with other projects (also thanks to CW operation), ensuring that there are no problems connected to space-charge effects.

However, the approximations in modelling a real linac with simulation codes can only lead to very preliminary conclusions as far as safety aspects are concerned. The following table is directly derived from the precise studies made in the frame of the SPL and CONCERT [52] projects, and gives an order of magnitude of the thickness of the radiation shielding needed at the high-energy (1-GeV) end of the linac. The shielding is here considered as a combination of a concrete shielding close to the accelerator with an additional earth shielding around the concrete. The given values ensure that people working around the accelerator can be classified as non-exposed workers. (The Euratom limit is 1 mSv/year, i.e. an average dose of 0.5 μSv/hour assuming 2000 working hours per year). We assume here a continuous beam loss of 1 W/m during routine operation (values are also given for a 5 W/m loss).

Table 3.15: Radiation shielding.

Linear beam loss	Shielding thickness (for < 0.5 µSv/h dose)
1 W/m	5.5 m concrete OR 7.5 m earth OR 1 m concrete + 6 m earth
5 W/m	6.5 m concrete OR 8.5 m earth OR 1 m concrete + 7 m earth

Note that this kind of shielding should be quite thick enough, even in the case of an accidental beam loss: it is estimated that the loss of the 5-MW EURISOL beam at 1 GeV for 1 second would only induce a 2-µSv integrated dose (calculation in the case of the 5-W/m shielding). This shows that accidental beam losses should lead to a negligible increase of the average dose, since even with one accident of this type per day, the average dose would only rise from 0.5 µSv/hour to 0.58 µSv/hour.

3.3.7 R&D program

Several technological aspects related to the 700-MHz cavities are now being considered in different laboratories in both France and Italy (see figure 3.19). A simple stainless-steel helium tank directly braced to the niobium beam tube has been designed. A first single-cell cavity prototype (A105) incorporating this tank has been tested in a vertical cryostat, showing excellent results (see figure 3.9). A new cold tuning system, associated with a fine-tuning system based on piezoelectric actuators, is also under development.

During the coming year, the fabrication of several multi-cell (5-cell) prototype cavities of β=0.47 and 0.65, respectively, is scheduled. This is the major R&D activity in the present phase. These cavities, initially tested in vertical cryostats, will be equipped with helium tanks and cold tuning systems for tests on a horizontal cryostat (CRYHOLAB) in order to study the cavities behaviour under accelerator operating conditions.

The tests at high RF power levels require the development of a power coupler adapted to these cavities. Some preliminary work has been done at Saclay on this subject [53]. At the same frequency of 700 MHz, the APT-AAA project has developed a new power coupler that has been tested at room temperature reaching an impressive performance of 1 MW in CW mode (500 kW when cooled at liquid nitrogen temperature). At a different frequency (500 MHz) a power coupler is in routine operation at the KEK-B accelerator with a power level of 380 kW CW. This model has been chose by the SNS project and it will be adapted to the 805-MHz frequency. For the power range needed in the EURISOL project (7 to 50 kW) all these performances confirm the feasibility of such a component. Nevertheless, the development of a power coupler for EURISOL, or the adaptation of an existing model, remains an R&D subject of great importance for the next few years.

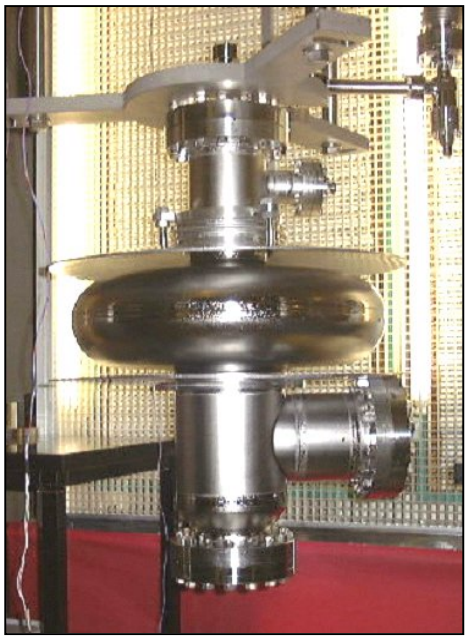

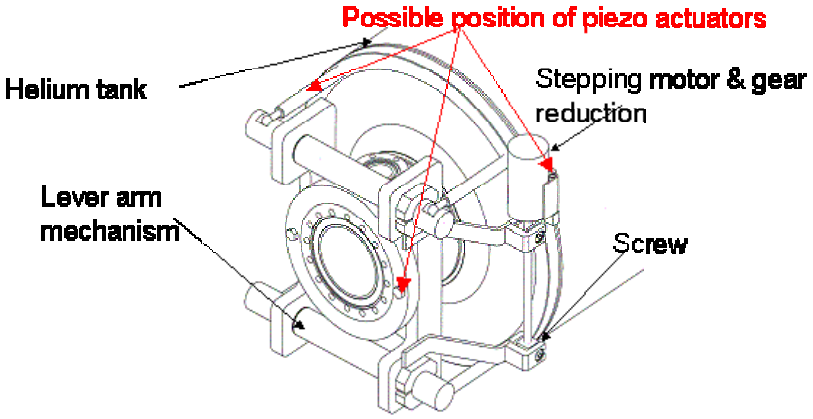

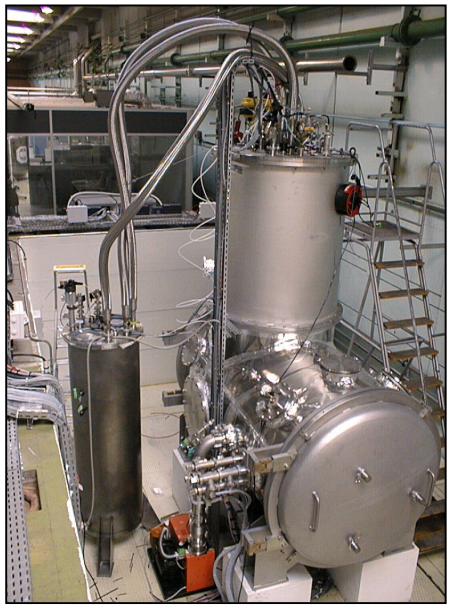

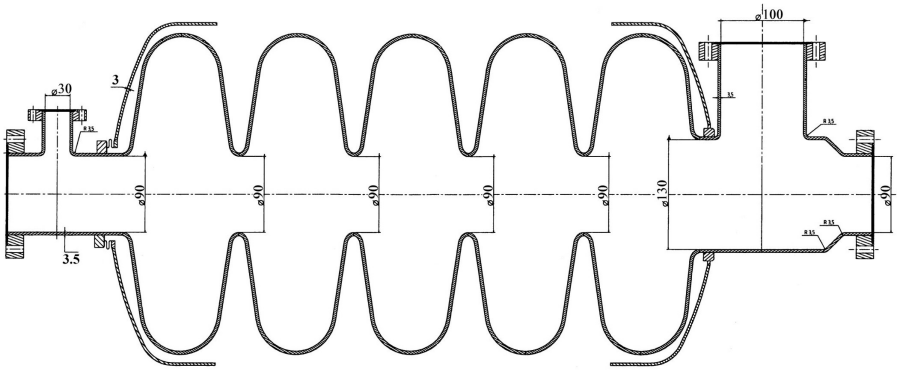

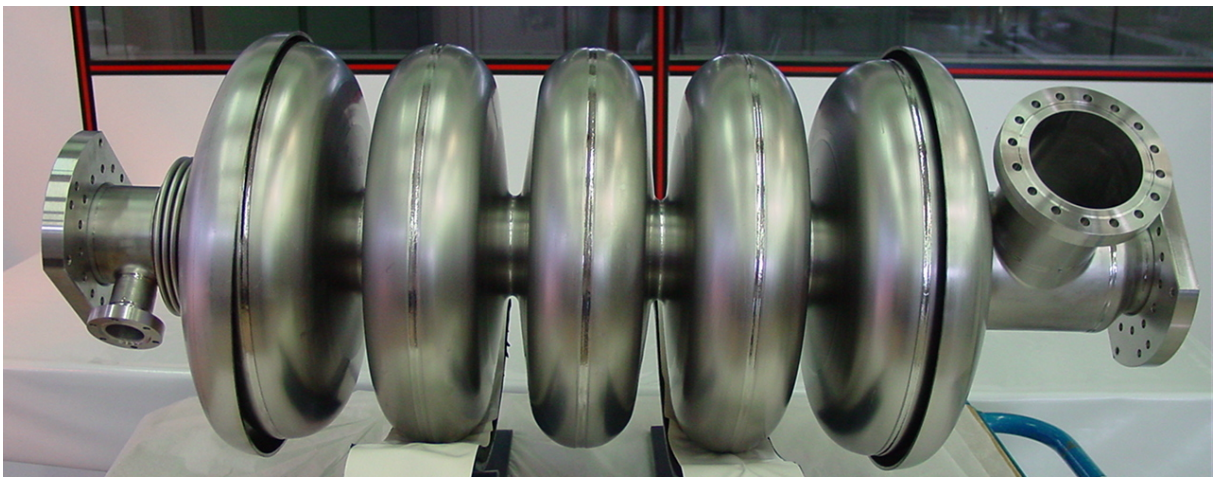

Fig. 3.19: (Top left:) Cavity A105 with its brazed stainless steel helium tank. (Top right:) Tuning system. (Centre left) Sketch of the β=0.65, 5-cell cavity. (Centre right). The horizontal cryostat CRYHOLAB (CEA/CNRS) installed at Saclay. (Bottom:) The completed β=0.6, 5-cell cavity recently fabricated at CERCA.

3.3.8 Preliminary cost estimate

This preliminary cost estimate is based on more elaborated studies like SNS, ESS, ASH and SPL, and reaches a total amount of less than 90 M€ (See table 3.16). It covers the investment on the main components of the high-energy section of the EURISOL driver up to 1 GeV. The infrastructure, the buildings, the manpower and contingency factors are not yet included in this estimate. Note that a 2-GeV upgrade would need an investment of around 65 M€ (components cost only).

Table 3.16: Component cost estimate for the 85-MeV–1-GeV, 5-mA CW EURISOL linac.

Components	Number	Unit Price (M€)	Total (M€)	Comments
Cryomodules				
* Cavities	134	0.15	20.1	Cavities including couplers, tuners, etc.
* Cryostats	45	0.25	11.3	He tanks, thermal shields, instrumentation
RF System				
* RF Sources	134	0.07	9.4	Tubes & circulators
* Power Supplies	8 MW	0.7	5.6	
* Low Level	134	0.05	6.7	
* Waveguides	300 m	0.003	0.9	
Cryogenic system 2K				
* Refrigerator	4.5 kW	-	19.9	Cold boxes, compressors, storage
* Transfer lines	350 m	0.01	3.5	
Vacuum				
* Warm sections	45	0.03	1.4	Pumps, valves, beam tubes
Focusing				
* Quadrupoles	90	0.05	4.5	Including power supplies
Beam Diagnostics	-	-	1.5	
Controls	-	-	4.0	
TOTAL			**88.8 M€**	

A preliminary operating cost estimate is also given for the whole linac in table 3.17 (overleaf). This costing is based on an operational time of 80% and on an electricity cost of 0.055 €/kW.h. Staffing and maintenance costs are not included in this estimate.

Table 3.17: Electricity cost estimate for the whole 1-GeV, 5-mA CW EURISOL linac.

	AC power for RF (MW)	**AC power for cryogenics (MW)**	**Electricity cost (M€/year)**
Low-energy section	2.1	-	0.8
Intermediate section	1.0	0.3	0.5
High-energy section	8.5	3.2	4.5
TOTAL	**11.6**	**3.5**	**5.8 M€/year**

4 Heavy Ion Capability of the Proton Driver

4.1 General considerations

A linear accelerator is designed for a given velocity profile of the ions. In particular, the phase of the RF fields in the accelerating structures is set according to this velocity profile. Moreover, the accelerating structures themselves have an optimum efficiency matched to the velocity profile. [A transit-time factor (TTF) of less than about 0.4 is inefficient.] All this means that if a linac is optimised for protons, it will definitely not be optimised for $A/q > 1$.

On the other hand, it is possible to build a linac which can accelerate ions with values of A/q in a quite a large range, but such a linac will be longer, more costly, and less efficient than if optimised for a single type of ion (see the 3 scenarios outlined in section 4.2).

In order to be able to cope with heavy-ion acceleration in the EURISOL proton driver, two basic specifications have to be taken into account:

- The accelerating structures have to be carefully selected and, in particular, the ***number of gaps per structure has to be kept small*** so as to retain ***a large velocity acceptance***. The TTFs in figure 4.1 clearly show that an increased number of gaps results in a much narrower velocity acceptance. This effect is predominant at low energy. At high energy, however, the number of gaps per structure can be increased more easily (figure 4.2).
- The phases in the successive accelerating structures have to be adequately controlled, which means that ***the number of structures driven with a fixed phase has to be kept small***. The more structures driven with the same phase, the smaller is the velocity acceptance (figure 4.3).

It is a remarkably lucky circumstance that these two requirements have in fact been satisfied in the design of the EURISOL proton driver: 2-gap structures are used in the intermediate section (5–85 MeV), and each cavity or resonator in the whole linac (5 MeV – 1 GeV) is driven with an independent RF power source. However, the same initial velocity for all types of ions is needed at the entrance of the phase-driven linac (at 5 MeV). It is therefore necessary to construct a second RFQ injector, designed for heavy-ion operation, which will in general be longer and less efficient.

4.2 Description of a few scenarios

We have considered and analysed the possibility of accelerating heavy ions with the 1-GeV EURISOL proton driver described in section 3, with the minimum change and cost increase.

We identified three scenarios:

1) **The acceleration of heavy ions, $A/q = 2$ & 3 up to the end of the proton linac intermediate section (85 MeV proton energy).**
2) **The acceleration of heavy ions with $A/q = 2$ up to the end of the main linac (to 1 GeV).**
3) **The acceleration of heavy ions with $A/q = 3$ up to 100 MeV/u, with a modification of the proton linac architecture.**

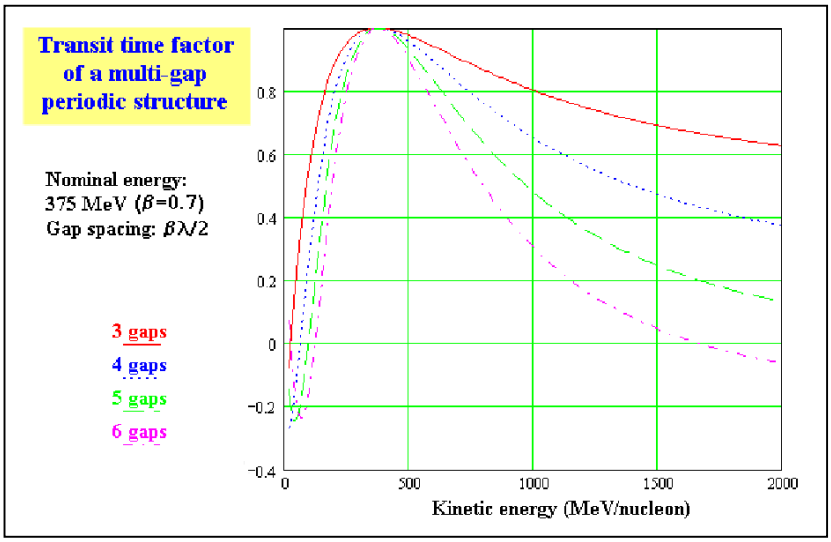

Fig. 4.1: Velocity acceptance of a multi-gap periodic structure (3, 4, 5 & 6 gaps) around 375 MeV.

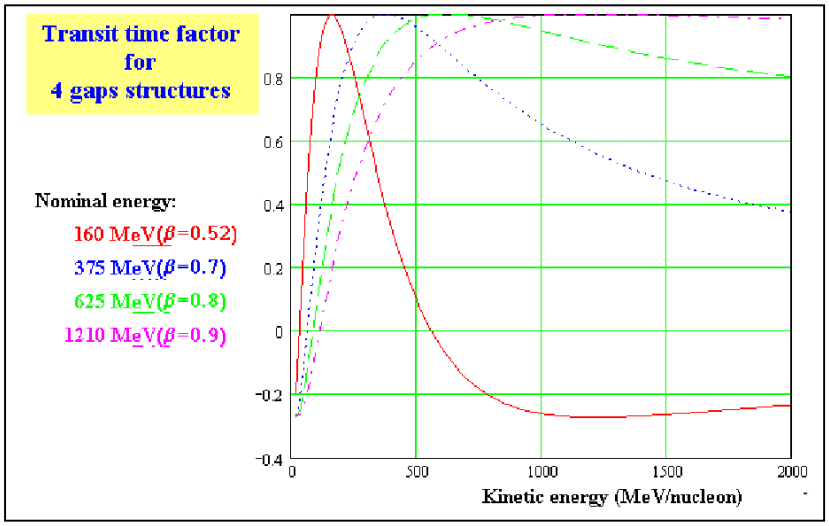

Fig. 4.2: Velocity acceptance of a 4-gap periodic structure at different energies.

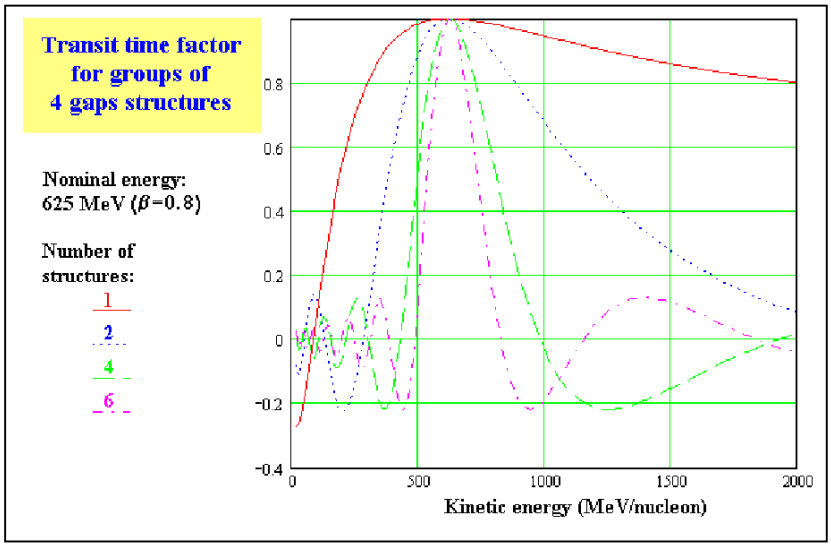

Fig. 4.3: Velocity acceptance of a 4-gap periodic structure for different number of structures driven at the same phase.

First scenario:

In the first case, one has to built a second injector, able to cope with A/q = 3, and to inject such a beam at the convenient energy (about 7 MeV/u) in the intermediate energy (superconducting) linac. In the SPES proposal [54], an injector operating at 176 MHz and composed of a 1.7 MeV/u RFQ plus 18 QWRs has been conceived for this application and quotes a cost of approximately 14 M€. At the end of the intermediate section, heavy ions with 43 MeV/u for A/q = 2 and 28 MeV/u for A/q = 3 would be available for experiments in this scenario.

Second scenario:

In the second case the main linac is used for ions with A/q = 2. This is possible if the field in the high-energy section of the linac is increased so that the surface magnetic field goes from 50 to 60 mT. The final energy is thus about 500 MeV/u. In figure 4.4 we show the transit-time factor along the main linac. This curve has to be compared with the nominal case of protons at 50 mT shown in the same figure.

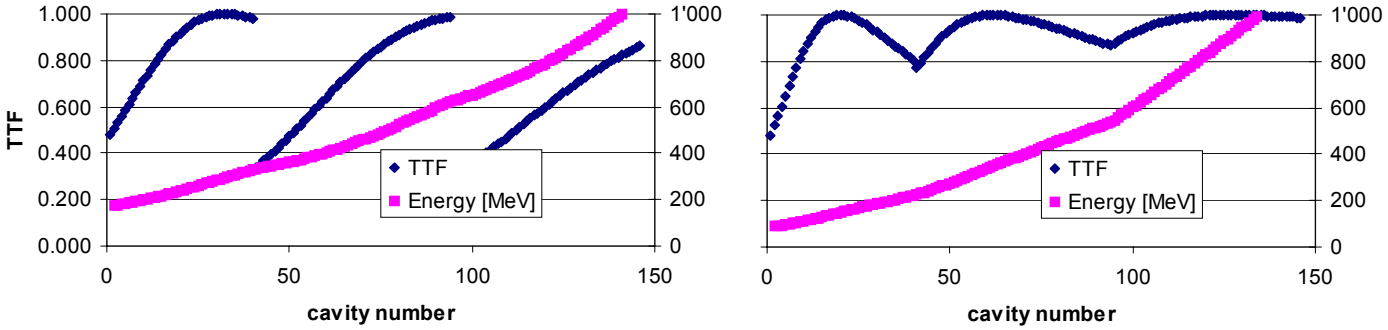

Fig. 4.4: Transit-time factor and energy evolution through the high-energy section for A/q = 2 ions (left) and A/q = 1 ions (right).

Note that to achieve this result, it is necessary to double the intermediate part (so as to attain the same velocity at the input of the main linac), as schematically shown in figure 4.5. In this case the capability of independently phasing the cavities of the intermediate-energy linac is not used; and this part of the linac, working with a fixed beta profile and half the accelerating field for protons, can be either normal-conducting or superconducting. The approximate cost of this option is obtained by summing the ion injector of the previous paragraph plus the doubling of the intermediate linac section, for a total of at least 37 M€.

Third scenario:

The third scenario is the least certain. One could extend the intermediate part of the proton linac (with cavities with a small number of gaps, QWR or spoke) up to 300 MeV. For example, about 120 two-gap cavities with β=0.45, 6 MV/m accelerating field over an effective length of 0.36 m, could be developed and used for this application. The main linac would begin only at this point, without the use of the elliptical β=0.47 cavities. The intermediate-energy linac could accelerate a beam with A/q = 3 up to about 100 MeV/u, and a beam with A/q=2 up to 150 MeV/u. Note that the elliptical cavity part of the linac is in this case used only for protons (figure 4.5).

This last option requires much more study to prove its feasibility, and in any case has deep implications for both the architecture and cost of the whole driver.

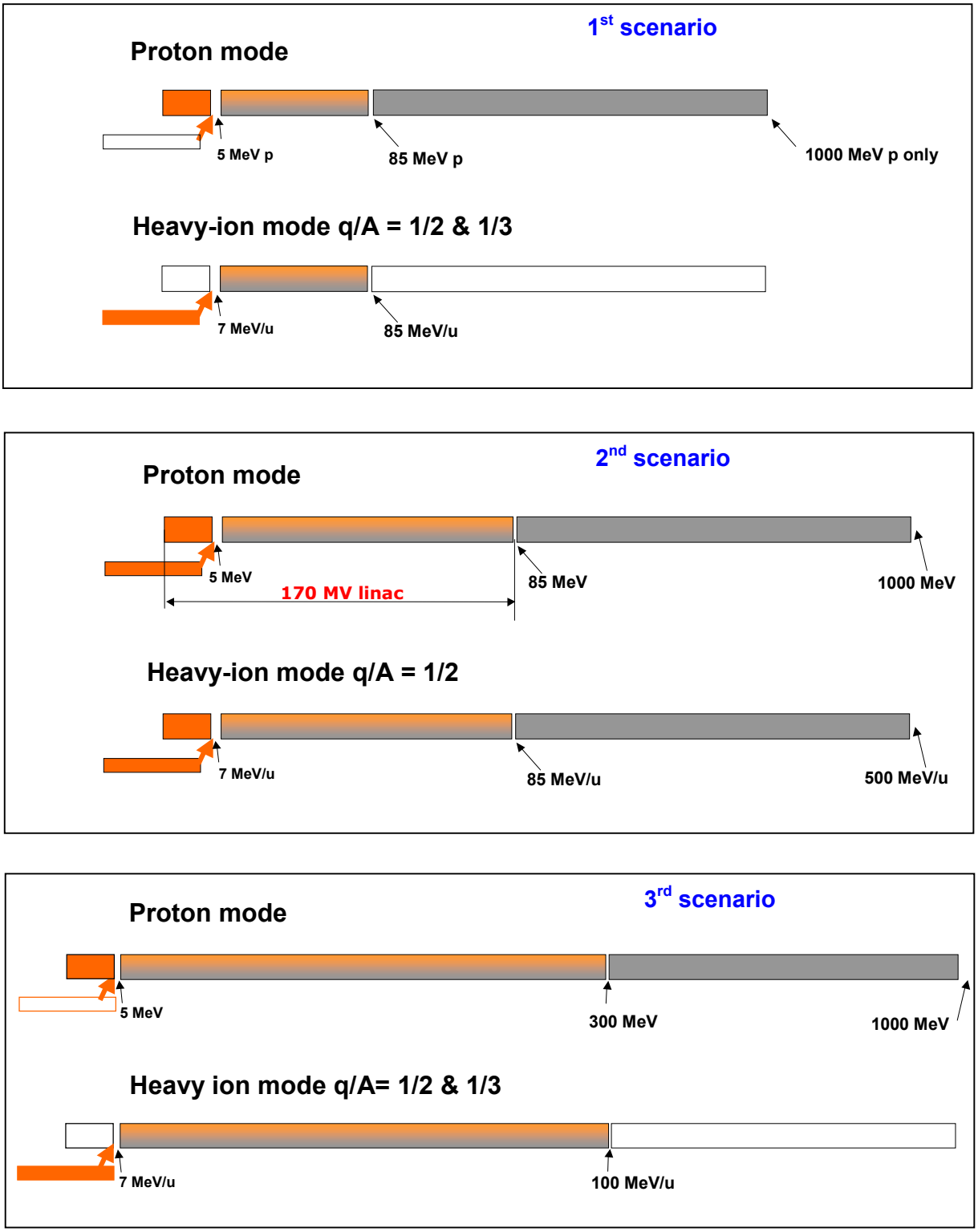

Fig. 4.5: Schemes for the three heavy-ion acceleration scenarios described in the text.

5 Driver Accelerator Operating Mode

The choice of operating mode was an important issue for the EURISOL Driver Accelerator Task Group, since a detailed and efficient study of the accelerator could not be done without knowing if the beam would be pulsed or not. In this section, we discuss some of the main points in order to clarify the situation in the EURISOL context, focusing on the proton driver accelerator.

5.1 Operating current

For the neutron-production mode (2-step mode with a spallation target), the EURISOL driver will need a maximum proton beam power of approximately 5 MW (i.e. a 5-mA average current at 1 GeV). In pulsed operation, the peak current will be higher than in CW operation (~100 mA in a typical multi-purpose linac). This leads to facts such as:

- ***higher sensitivity to space-charge effects in pulsed mode*** (this point is especially important at low energy);
- ***higher peak power requirements in pulsed mode.*** If we take the case of a 700-MHz 5-cell β=0.65 cavity (with r/Q=150 Ω, circuit definition) running at B_{pk}=50 mT (E_{acc}≈10 MV/m) and φ=-30°, the maximum RF power capability must be about 50 kW CW or 1 MW pulsed per cavity (to ensure comfortable operation margins). Apart from RF power source considerations, the most important point here is the impact on power coupler requirements. Considering the actual state of the art, it is clear that the development of a 50-kW power coupler remains an easy task, whereas the development of a 1-MW power coupler exceeds the limits of present-day technology and is actually a tremendous challenge. Considering this, the choice of a pulsed machine at 100-mA peak current would have a serious impact on the overall machine reliability.

5.2 Lorentz-force detuning

During operation, the electromagnetic field pressure exerted on the cavity wall induces a resonance frequency change, known as the Lorentz-force detuning. This shift is quite small (Hz to kHz range) but can put the resonance out of reach of the phase-lock-loop system. This effect is not crucial at all in CW mode because the shift remains constant during operation, but it is definitely a serious issue for pulsed operation because this detuning induces cavity frequency fluctuations. Owing to Lorentz detuning, ***cavities under pulsed operation*** need two main additional requirements:

- ***Additional mechanical stiffening*** of the cavity walls must be realised so as to limit the frequency shift to less than half the full-width half maximum of the cavity – generally a few Hz/(MV/m)². Note here that the lower the cavity beta, the more stiffening is required.
- ***An efficient feedback system*** has to be built around cavity and transmitter to fight these detuning consequences. This feedback system reduces the effect of Lorentz detuning by regulating the RF input power, but at the cost of ***extra RF power***. This extra power ΔP can be roughly estimated from:

$$\frac{\Delta P}{P} = \left(\frac{\Delta f_L}{f_{1/2}} \right)^2$$

where Δf_L is the Lorentz force frequency shift, $f_{1/2}$ is the loaded cavity full bandwidth ($f_{1/2}=f/Q_L$) and P is the nominal RF power.

In a EURISOL pulsed machine (100 mA peak), the loaded Q-value of a 5-cell 700-MHz β=0.65 cavity is about $Q_L = V_{acc}/2(r/Q)\cdot I \cos\varphi \approx 3.10^5$, which corresponds to a cavity bandwidth of around 2.5 kHz. For a realistic Lorentz coefficient of 8 Hz/(MV/m)² – which means an 800-Hz detuning at E_{acc}=10 MV/m – **the extra power required will be about 12% of the RF peak power**.

It is important to note that this extra power depends strongly on the peak beam current: for a lower current, the cavity bandwidth becomes narrower (and Q_L higher), and the Lorentz detuning consequences can become very problematic. With pulsed operation at 20-mA peak current, for example, keeping extra power below 15% RF peak power means lowering the Lorentz coefficient below 1.5 Hz/(MV/m)², which represents a real challenge in terms of cavity stiffening.

5.3 Power efficiency

A preliminary study presented in table 5.1 shows that at nominal power (for a 5-MW stand-alone machine, and assuming that there are no RF-system or beam errors), the total efficiency remains very good (around 40%) in both cases.

Table 5.1: Comparison of power efficiencies in the high-energy section (β=0.65 section).

Parameter	CW operation	Pulsed operation – stand-alone
Nominal current	5 mA	100 mA peak *(5 % duty cycle, 1 ms pulse, 50 Hz)*
Q_L needed *(cavity field rise time)*	5.5×10^6 *(1.7 ms at nominal power)*	2.8×10^5 *(90 μs at nominal power)*
Cavity bandwidth	130 Hz	2.51 kHz
RF beam loading	31.1 kW	31.1 kW average *(621.4 kW peak)*
Extra RF power [a]	1.2 kW	3.9 kW average
Cavity loading	0	3.0 kW average
Total RF power needed	32.3 kW	38.0 kW average *(692.9 kW peak)*
RF-to-beam efficiency	**96.3%**	**81.9%**
Dynamic losses at 2K	17.9 W *(17.2 W for cavity)*	5.4 W average *(1 W for cavity)*
Static losses at 2K	2.9 W	5.9 W
Total load at 2K [b]	20.8 W *(1.6 W for power coupler)*	11.3 W average *(8W for power coupler)*
Total AC efficiency [c]	**40.9%**	**40.8% [d]**

Note: All powers quoted per 700-MHz β=0.65 cavity at $\beta=\beta_g$, with no RF-system or beam errors.

a: Including Lorentz detuning (k_L = 8 Hz/(MV/m)²) and microphonics (+/-25Hz) compensation extra powers.

b: Assuming a cavity $Q_0=1\times10^{10}$ at 2K, static losses and coupler losses estimated from APT & SNS studies.

c: Assuming η_{cryo}=0.1% at 2K and a AC to RF efficiency of 65%×90%.

d: Note that for a multi-purpose machine (100 mA peak, 25% duty cycle), the efficiency is higher (around 45%).

To first order, there is ***no significant difference between efficiency in CW mode and in pulsed mode***: there is a balance between the RF extra power needed in pulsed operation (mainly for Lorentz-force compensation and cavity loading before the pulse) and the more important cavity dynamic losses in CW mode (100% RF duty cycle). That means that, in the final analysis, the difference between CW and pulsed operation efficiency will be determined mainly by the real performance of the components, and especially of the ***RF control-system efficiency***, the ***power-coupler performance***, and the ***cavity sensitivity to frequency variations***.

5.4 Commissioning

During the commissioning of such a machine, a pulsed operation (pulsed beam) must be implemented for test purposes. But this does not mean that the RF system also has to be pulsed, as in a fully-pulsed machine. The commissioning of a CW machine can easily be handled by adjusting the RF power, *without pulsing it*, in order to keep the cavity voltage constant (see figure 5.1). If during the pulse, RF power P_{nom} is required to feed the beam, then between the pulses, the cavity voltage is kept constant by injecting RF power $P_{nom}/4$. (Note that this power is fully reflected).

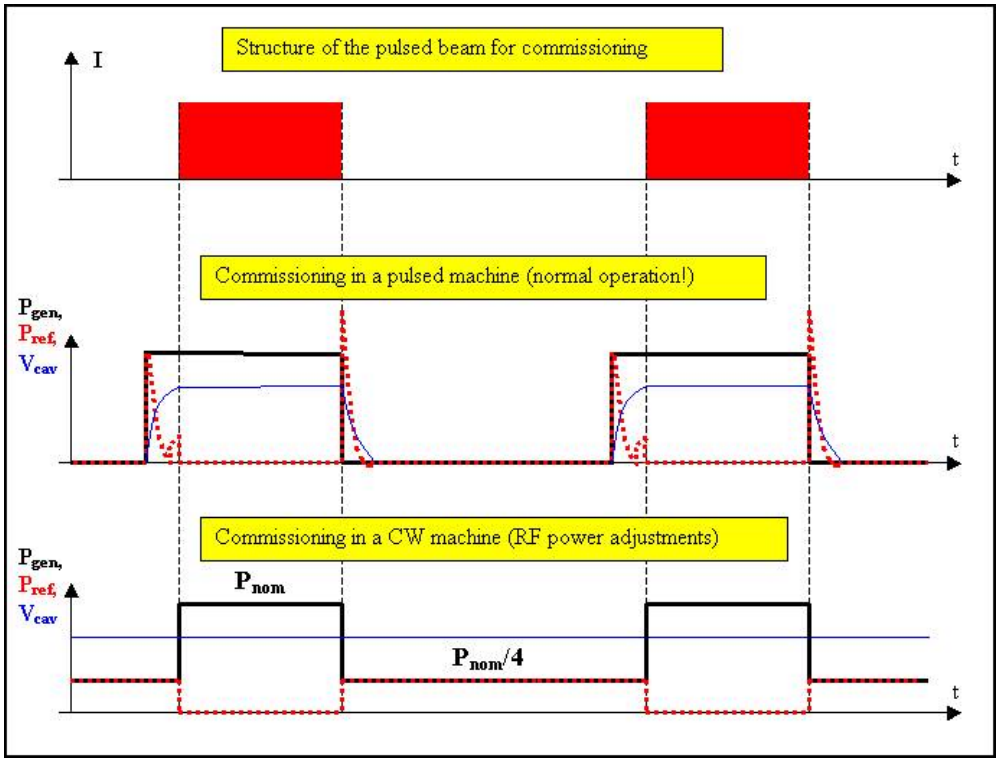

Fig. 5.1: Handling of a pulsed beam (for commissioning) with a CW machine.

5.5 Beam power flexibility

The ability to make beam power adjustments can be very useful because it opens up many opportunities for the user. This can be done by changing the beam's final energy (by cutting off some of the last cavities and re-adjusting the fields in the last quadrupoles, or switching on some dipole magnets at the desired energy), and/or by changing the beam current (i.e. the nominal current and/or the duty cycle, and re-adjusting the RF system). In the EURISOL layout, this is important, since 2 production modes must be considered: the 2-step 'neutron' mode (with a spallation target and a 5-MW beam), and the 'direct' proton mode (with a 0.5-MW beam).

In section 5.3, we considered the case of the main 'neutron' mode of production, with a 5-MW beam. Running with the same machine in the 'proton' mode with a 0.5-MW beam can easily be managed, e.g. by simply lowering the beam current while keeping the final energy constant:

- In CW operation, the current is lowered by a factor of 10 from 5 mA to 0.5 mA.
- In pulsed operation, the pulse length is shortened from 1 ms to 100 μs.

One should note here that the beam power flexibility does not really depend on the beam operation mode (CW or pulsed) but on the kind of accelerator desired: as can be seen in the table below, the flexibility is maximum in a stand-alone machine (in both CW or pulsed operation), whereas in a pulsed multi-purpose machine, only the duty cycle can easily be changed (refer to section 5.7).

Table 5.2: Flexibility of the driver accelerator.

Adjustment required	Stand-alone machine		Multi-purpose machine
	CW operation	Pulsed operation	Pulsed operation only
Current	YES	YES	NO
Final energy	YES	YES	NO (except using magnetic insertions - see section 5.6)
Pulse length	YES	YES	YES

5.6 Multi-mode running

We have just seen that, because of beam power flexibility, a driver can run with different production modes (different final energies, proton or neutron modes) with both CW and pulsed operations. However, in addition, one can envisage running these ***different production modes simultaneously***:

- Pulsed operation is here particularly well adapted to this purpose: each pulse can be divided in micro-pulses, each micro-pulse being directed (with magnets) to the desired target at the desired energy, exactly like in a full multi-purpose project.
- In CW operation, this can also be done using very long pulses (of about a few seconds), each such long pulse being also being directed to any desired target.

5.7 The multi-purpose facility option

The integration of EURISOL into a large multi-purpose facility can be interesting because it allows sharing of the cost of the driver accelerator between the different communities.

In this type of machine, the peak current and the final energy are fixed; the beam specifications for each application are mainly driven by pulsed length adjustments (see figure 5.2 – courtesy of the CONCERT study).

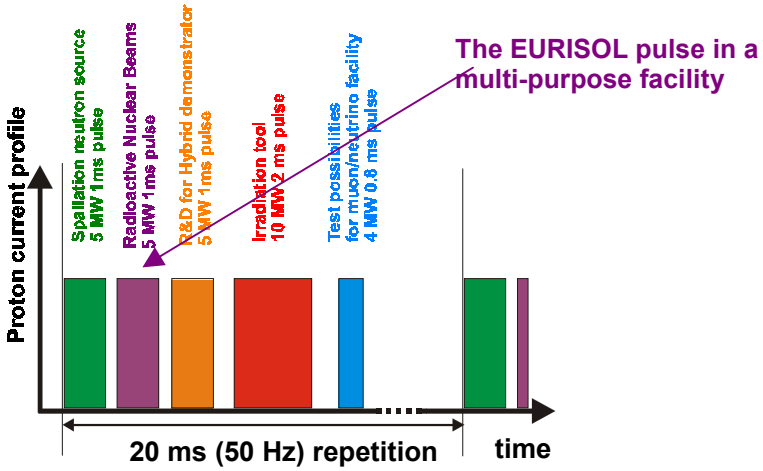

Fig. 5.2: Pulsed beam structure in a multi-purpose facility. (From the CONCERT study.)

5.8 High-order mode

In CW operation, high-order modes (HOM) may build up in the cavity only in the very unlucky case where its frequency happens to be an exact multiple of the bunch frequency. A careful analysis [55] shows that the probability of occurrence of HOM build-up is extremely low in a superconducting linac running under CW operation. We thus conclude that there is no need for specific HOM couplers for EURISOL superconducting cavities if operated under CW operation.

In pulsed operation, the situation is slightly different since the contribution of the pulse modulation leads in additional resonant build-ups. The probability of high-order modes of excitation by the beam is thus clearly more important in pulsed operation than in CW operation.

5.9 Summary

For a stand-alone EURISOL driver, the CW operation is preferred: reliability is maximum (lower peak power), the Lorentz forces problem vanishes in the accelerating cavities, and the R&D effort is significantly lowered (especially for the development of power couplers and design of the RF feedback system). Finally, CW operation leads to a simpler machine (probably with lower cost) ensuring very good efficiency, large flexibility, and retaining the possibility of running both proton (0.5-MW) and neutron (5-MW) production modes, or/and running with a stepwise variable energy (or even all simultaneously using very long pulses).

On the other hand, ***for a multi-purpose driver for EURISOL*** – or if many different production modes and targets must run at the same time – ***pulsed operation is preferred***.

Finally, the CW operation was chosen for the EURISOL drivers (for both protons and electrons), after considering the following points:

- A time structure as close to CW as possible is desirable from the point of view of target lifetime, though a repetition rate of 50 Hz is still acceptable.
- An important argument is that the EURISOL project could drive a strong R&D program on superconducting linacs, for both intermediate and high energies; this implies that CW operation at low current is globally preferred to pulsed operation at high current, since with today's state-of-the-art technology (e.g. the SNS, CONCERT studies), pulsed operation restricts one to using a room-temperature linac up to the beta=0.65 section (200 MeV).

6 Conclusion

This study has provided the technical solutions for suitable driver accelerators for a second-generation radioactive beam facility in the framework of the EURISOL concept.

The baseline option, a 1-GeV, 5-MW CW proton linac, extendable to an energy of about 2 GeV, has been investigated in some detail. It consists of a room-temperature ECR+RFQ injector, an intermediate-energy (5–80 MeV) section of independently-phased SCRF cavities and a high-energy section of elliptical cavities. The cost estimate for this accelerator is 120 M€, not yet including infrastructure, buildings and contingencies, for which we propose that a rough evaluation should be made for the project as a whole. The construction time is estimated to be between 5 and 7 years, the manpower supposedly being provided by collaborating European laboratories, which may need to strengthen their staff for this purpose.

The following major points have been identified:

- The injector section is an easy extrapolation (in fact a down-scaling) from projects presently under construction in Europe.
- The high-energy section uses structures that are within the present mainstream developments of low-β elliptical SCRF cavities. For the forthcoming European PCRD programme, the EURISOL community could certainly collaborate in a synergistic way with other foreseeable activities (XADS, ESS, ν-factory). In this context, the construction of full-scale prototypes of cryomodules for the β-values required by the various projects should be envisaged.
- The intermediate-energy section will use, a priori, independently-phased SCRF cavities of several types. This rather new technology still needs much important R&D effort. However, EURISOL can (and should) join and reinforce the research that recently has been launched in Europe. The room-temperature DTL solution, while less attractive from the point of view of efficiency, cost and flexibility, still exists as a back-up option.
- The 1-GeV linac can be upgraded, in the most straightforward way to an energy of 2 GeV by increasing the number of β=0.85 SCRF cavities. Such an upgrade would need an investment of around 65 M€.
- The CW mode of operation is preferable for the stand-alone driver, for a number of reasons that have been stated elsewhere. If the driver were to be shared in the context of a multi-purpose facility, then pulsed operation would be required. This is acceptable for EURISOL, provided that (a) the repetition-rate is sufficiently high, (b) the average beam intensity meets the demands of the ISOL users, and (c) that the beam availability for EURISOL component is not compromised.
- The proton linac has the ability to accelerate heavy-ions to some extent, notwithstanding the need for a dedicated injector accelerator. Owing to the principle of independent phasing and some margin in the maximum magnetic field of the elliptical cavities, acceleration of $A/q = 2$ ions is potentially feasible, up to 500 MeV/u. The necessary modifications would require an additional investment of at least 35 M€. A priori, similar electrical beam current as for proton operation can be envisaged since to first order this is defined only by the available RF power. Acceleration of $A/q = 3$ ions would need significant design modifications which have not been fully investigated. However, it is clear that, for

this case, a major part of the linac would no longer be cost-optimised for proton acceleration. It will also be necessary to investigate whether specific shielding is necessary for the radiological protection aspect.

As a driver for fission-products only, a superconducting 50–70-MeV, 20–30-mA electron linac has been studied. The cost for such an accelerator has been estimated to be 20 M€ (including infrastructure and buildings), a comparatively modest investment. More generally, high-intensity electron accelerators can be of interest for the upgrading of existing radioactive beam facilities.

When comparing photo-fission to the spallation process, the neutron cost is about 30 times higher in terms of the number of photo-fission events, while the accelerator cost is significantly lower. Therefore, for the same number of fissions, a higher electron intensity (and consequently beam power) will be needed due to the lower efficiency. Thus, above a given neutron flux, the spallation process will be preferred, while for the lower fluxes the photo-fission process will tend to be much cheaper. This can immediately be seen from figure 6.1 where, for a given neutron flux, the cost of an electron machine as well as a proton accelerator have been estimated. Note that this is the bare machine cost and does not include manpower or buildings (which are certainly even cheaper for the electron machine). It appears that for fluxes exceeding 10^{17} n/s, the spallation process will start to appear more effective while below 10^{16} n/s, the photo-fission process is cheaper, even though the beam power required is higher. Thus, if we restrict the aim to a fission rate of only 10^{15} fissions/s, an electron accelerator may be considered for the EURISOL fission-product-only driver accelerator. However, these considerations also need to be complemented by technical studies related to the feasibility of fission targets which can withstand such fluxes.

For these reasons, t***he proton driver is also the solution of choice*** for fission products for fluxes somewhere above 10^{16} n/s. The electron driver is an interesting and somewhat cheaper back-up solution, notwithstanding the target issue.

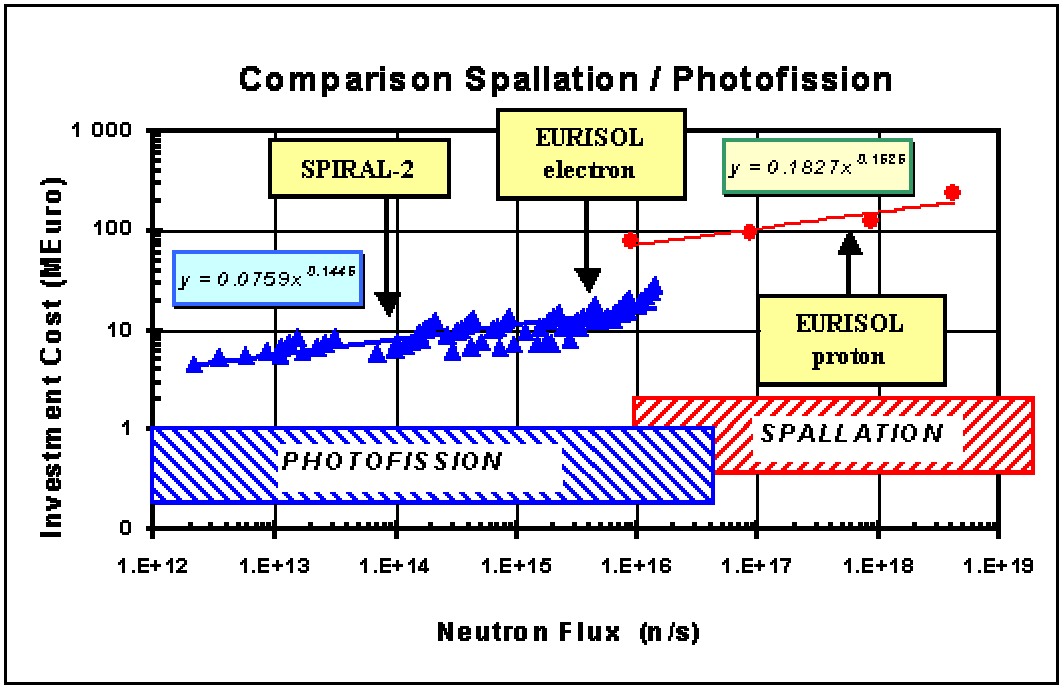

Fig. 6.1: Comparison of the driver accelerator investment cost for the photo-fission and the spallation processes, as a function of the neutron flux produced in the respective targets.

6.1 Recommendations

The Driver Accelerator Task Group concludes this report with the following facts and recommendations:

- **The EURISOL base-line driver accelerator, a 1-GeV, 5-MW CW proton facility, with a possible upgrade to 2 GeV, has remarkable synergies in components and R&D needs with other high-intensity projects. The proposed solution is thus in the mainstream of today's accelerator development.**
- **The demonstration of the injector accelerator, up to about 10 MeV, relies on existing projects like IPHI or the TRASCO injector. Therefore, it is important that full funding for these R&D projects is continued.**
- **Two items have high R&D priority: (a) construction of complete prototype accelerator sections for low-β elliptical SCRF cavities; (b) development of prototypical spoke, quarter-wave and re-entrant cavities with associated auxiliary RF components, to be tested with beam from existing facilities.**
- **The funding for these identified R&D needs for the EURISOL driver accelerator should be proposed, within the frame of the European Commission's 6th PCRD, in a co-ordinated manner with other projects, where applicable.**
- **Assuming that it is possible to establish common R&D programmes with other projects, it should be investigated whether common designs could be adopted. Important cost saving can be anticipated from this action.**
- **Such a common and 'synergistic' R&D programme should also provide the opportunity to investigate whether additional saving can be achieved by sharing the driver accelerator. From the technical point of view, pulsed driver accelerators provide a priori sufficient beam power for time-sharing the beam between two or even more users. However, at present it is still too early to draw conclusions about the opportunities for such an approach.**

References

[1] See the various laboratories' general web sites: http://www.cea.fr/, http://www.cern.ch/, http://www.ganil.fr/, http://www.lnl.infn.it/ and http://ipnweb.in2p3.fr/.

[2] See http://nfwg.home.cern.ch/nfwg.

[3] See for example http://itumagill.fzk.de/ADS, http://trasco.lnl.infn.it/ and http://www.gedeon.prd.fr/.

[4] See for example http://www.pnl.gov/atw and http://aaa.lanl.gov/atw.

[5] See http://inisjp.tokai.jaeri.go.jp/ACT95E/11/11-1.htm.

[6] *"A European Roadmap for Developing Accelerator Driven Systems (ADS) for Nuclear Waste Incineration"*, Technical Working Group on Accelerator-Driven Systems, May 2001, http://www.neutron.kth.se/TWG22/download/ads.pdf.

[7] See http://www.sns.gov/.

[8] See http://jkj.tokai.jaeri.go.jp/.

[9] See http://www.ess-europe.de/.

[10] T.Adachi et al., PAC 2001, P.3254 and refs. therein.

[11] A. Veyssière et al., Nuclear Physics, **A199**(1973)45

[12] Y. Oganessian, in Proc. Radioactive Nuclear Beams 2000, Divonne-les-Bains, France, April 2000.

[13] H. Safa et al., *"Photo-fission for the SPIRAL-2 project"*, ISOL '01, Oak Ridge, USA, March 2001.

[14] F. Ibrahim et al., *"Photo-fission for the production of radioactive beams: experimental data from an on-line measurement"*, Sept. 2001 http://www.ganil.fr/eurisol/TargetGroupMeetings/Faadi-photofission-cern.pdf.

[15] D. Goutte, *"Spiral & Spiral II"*, EURISOL Town Meeting, Orsay, France, Nov. 2000. http://www.ganil.fr/eurisol/townmeetingorsay/dominiquegoutte.pdf.

[16] A.C. Mueller, *"High-Power Accelerators and Radioactive Beams of the Future"*, Nuclei Far from Stability and Astrophysics, **7-17**, 2001.

[17] M-G. Saint-Laurent et al., *"Spiral Phase II"*, European RTT, Final report, Contract Number ERBFMGECT980100, September 2001, http://www.ganil.fr/spiral2/Spiral_PhaseII.pdf.

[18] B. Aune et al., *"The Superconducting TESLA Cavities"*, Phys. Rev. ST-AB, vol. **3** (2000), http://prst-ab.aps.org/pdf/PRSTAB/v3/i9/e092001.

[19] P. Leconte et al., "MACSE", DAPNIA / SEA 92-09, Saclay, France (1992).

[20] H.V. Smith et al., *"Status report on the low energy demonstration accelerator (LEDA)"*, XX Int. Linac Conf., Monterey, USA, August 2000, http://www.slac.stanford.edu/econf/C000821/TUD14.pdf .

[21] P-Y. Beauvais et al., *"Status reports on the Saclay high-intensity proton injector project"*, EPAC 2000, Vienna, Austria, June 2000, http://accelconf.web.cern.ch/accelconf/e00/PAPERS/THOAF202.pdf.

[22] See http://trasco.lnl.infn.it/.

[23] R. Gobin et al., *"New performances of the CW high-intensity light-ion source SILHI"*, EPAC '98, Stockholm, Sweden, June 1998, http://accelconf.web.cern.ch/AccelConf/e98/PAPERS/MOP09A.pdf.

[24] G. Ciavola et al., *"First beam from the TRASCO intense proton source (TRIPS) at INFN-LNS"*, PAC 2001, Chicago, USA, June 2001, http://accelconf.web.cern.ch/AccelConf/p01/PAPERS/WPAH303.pdf.

[25] A. Pisent et al., *"TRASCO RFQ"*, Proceedings of the XX International Linac Conference, Monterey, USA, August 2000, http://trasco.lnl.infn.it/Document/trascorfq.pdf.

[26] M. Vretenar for the SPL Study Group, *"Conceptual design of the SPL, a high-power superconducting H- linac at CERN"*, CERN 2000-012, Dec. 2000, http://preprints.cern.ch/yellowrep/2000/2000-012/p1.pdf.

[27] H. Safa, *"Superconducting Proton Linac for Waste Transmutation"*, 9th Workshop on RF Superconductivity, Santa Fe, USA, Nov. 1999, http://laacg1.lanl.gov/rfsc99/WEA/wea005.pdf.

[28] A. Facco et al., *"Study on beam steering in intermediate β superconducting quarter wave resonators"*, PAC-2001, Chicago USA, June 2001, http://accelconf.web.cern.ch/AccelConf/p01/PAPERS/MPPH136.pdf.

[29] A. Facco et al., *"A Superconductive, Low Beta Single Gap Cavity for a High Intensity Proton Linac"*, Proc. XX Int. Linac Conf., Monterey, USA, August 2000, http://www.slac.stanford.edu/econf/C000821/THD11.pdf.

[30] G. Olry et al., *"Study of a spoke cavity for low-beta applications"*, 10th Workshop on RF Superconductivity, Tsukuba, Japan, Sept. 2001, http://conference.kek.jp/SRF2001/.

[31] A. Pisent et al., *"TRASCO 100 MeV High Intensity Proton Linac"*, EPAC-2000, Vienna, Austria, June 2000, http://accelconf.web.cern.ch/accelconf/e00/PAPERS/THP6B15.pdf.

[32] A. Facco et al. *"RF Testing of the TRASCO Superconducting Re-entrant Cavity for High Intensity Proton Beams "*, EPAC 2002, Paris, France, June 2002, http://accelconf.web.cern.ch/AccelConf/e02/PAPERS/THPDO022.pdf.

[33] A. Lombardi et al., *"The New SC Positive Ion Injector for the Legnaro ALPI Booster"*, XVIII Int. Linac Conf., Geneva, Switzerland, August 1996, http://linac96.web.cern.ch/Linac96/Proceedings/Monday/MOP30/Paper.pdf.

[34] F.L. Krawczyk et al., *"Design of a low-β, 2-gap spoke resonator for the AAA project"*, PAC 2001, Chicago, USA, June 2001, http://pacwebserver.fnal.gov/papers/Monday/PM_Poster/MPPH058.pdf.

[35] T. Tajima et al., *"Evaluation and testing of a low-β spoke resonator"*, PAC-2001, Chicago, USA June 2001, http://accelconf.web.cern.ch/AccelConf/p01/PAPERS/MPPH057.pdf.

[36] G. Olry et al., *"Design and industrial fabrication of β=0.35 spoke-type cavity"*, EPAC 2002, Paris, France, June 2002, http://accelconf.web.cern.ch/AccelConf/e02/PAPERS/THPDO035.pdf.

[37] G. Olry et al., *"R&D on spoke-type cryomodule"*, EPAC 2002, Paris, France, June 2002, http://accelconf.web.cern.ch/AccelConf/e02/PAPERS/TUPDO007.pdf.

[38] A. Pisent et al., *"Study of a Superconducting 100 MeV linear accelerator for Exotic Beam production"*, EPAC 2002, Paris, France, June 2002, http://accelconf.web.cern.ch/AccelConf/e02/PAPERS/THPLE041.pdf.

[39] V. Andreev et al. *"Study of a Novel Superconducting Structure for the Very Low Beta Part of High Current Linacs"*, EPAC 2002, Paris, France, June 2002, http://accelconf.web.cern.ch/AccelConf/e02/PAPERS/THPDO021.pdf.

[40] F. Scarpa et al. *"A 2.5 kW, Low Cost 352 MHz Solid State Rf Amplifier for Cw and Pulsed Operation"*, EPAC 2002, Paris, France, June 2002, http://accelconf.web.cern.ch/AccelConf/e02/PAPERS/TUPLE121.pdf.

[41] A. F. Zeller et al. *"A Superferric Quadrupole for use in an SRF Cryomodule"* LNL Annual Report 2001, INFN-LNL 181/02, http://www.lnl.infn.it/~annrep/readAN/2001/contrib_2001/254.pdf.

[42] J-L. Biarrotte et al., *"High-intensity proton SC linac using spoke cavities"*, EPAC 2002, Paris, France, June 2002, http://accelconf.web.cern.ch/AccelConf/e02/PAPERS/THPLE038.pdf.

[43] See http://www-dapnia.cea.fr/Sea/collabo/index.html.

[44] TESLA Technical Design Report, March 2001, http://tesla.desy.de/new_pages/TDR_CD/start.html.

[45] T. Tajima et al., *"Development of 700 MHz 5-cell superconducting cavities for APT"*, PAC 2001, Chicago, USA, June 2001, http://laacg1.lanl.gov/scrflab/pubs/APT/LA-UR-01-3140.pdf.

[46] C. Rode et al., *"The SNS Superconducting Linac System"*, PAC 2001, Chicago, USA, June 2001, http://accelconf.web.cern.ch/AccelConf/p01/PAPERS/ROPB008.pdf.

[47] F. Gerigk, *"Design of the superconducting section of the SPL linac at CERN"*, PAC 2001, Chicago, USA, CERN/PS 2001-050 (RF), June 2001, http://accelconf.web.cern.ch/AccelConf/p01/PAPERS/FPAH099.pdf.

[48] M. Mizumoto et al., *"Development of superconducting linac for the KEK/JAERI Joint Project"*, Proc. of the XX Int. Linac Conf., Monterey, USA, August 2000, http://lcdev.kek.jp/Conf/Linac2000/TUD09.pdf.

[49] G. Ciovati et al., *"Superconducting prototype cavities for the spallation neutron source (SNS) project"*, PAC 2001, Chicago, USA, June 2001, http://accelconf.web.cern.ch/AccelConf/p01/PAPERS/ROAA005.pdf.

[50] J-L. Biarrotte et al., *"704 MHz SC Cavities for a High Intensity Proton Accelerator"*, 9th Workshop on RF Superconductivity, Santa Fe, USA, Nov. 1999, http://laacg1.lanl.gov/rfsc99/WEP/wep005.pdf.

[51] P. Pierini et al., *"Cavity Design Tools & Applications to the TRASCO Project"*, 9th Workshop on RF Superconductivity, Santa Fe, USA, Nov. 1999, http://trasco.lnl.infn.it/Document/wep004.pdf.

[52] See http://web.concert.free.fr/.

[53] G. Devanz et al., *"Preliminary design of a 704 MHz power coupler for a high-intensity proton linear accelerator"*, EPAC 2000, Vienna, Austria, June 2000, http://accelconf.web.cern.ch/accelconf/e00/PAPERS/THP5B02.pdf.

[54] SPES technical design for an advanced exotic ion beam facility at LNL, A. Bracco and A. Pisent editors, LNL-INFN(REP) 181/02 (2002).

[55] J-L. Biarrotte, *"A statistical analysis of the danger induced by HOM excitation in a superconducting linac"*, PAC 2001, Chicago, USA, June 2001, http://accelconf.web.cern.ch/AccelConf/p01/PAPERS/MPPH137.pdf.

Addendum Driver Accelerator Task Group

Co-ordinator: Alex Mueller[1]

Task Group Members:
Eric Baron[2], Jean-Luc Biarrotte[1], Jean-Louis Coacolo[1], Michele Comunian[3], John Cornell[2], Alberto Facco[3], Shinian Fu[6], Roland Garoby[4], Tomas Junquera[1], Jean-Michel Lagniel[5], Marie-Hélène Moscatello[2], Guillaume Olry[1], Andrea Pisent[3], Henri Safa[5] and André Tkatchenko[1]

1 *IPN Orsay, France*
2 *GANIL, France*
3 *INFN, Laboratori Nazionali di Legnaro, Italy*
4 *CERN, Geneva, Switzerland*
6 *CEA Saclay, France*
6 *IHEP Beijing, China*

Acknowledgements

The contributions of B. Aune, S. Bousson, G. Devanz, R. Duperrier, G. Fortuna, H. Gassot, F. Gerigk, J. Lesrel, A. Mosnier, N. Pichoff, H. Saugnac, D. Uriot, J. Vervier and M. Vretenar during informal discussions are gratefully acknowledged.